Probabilistic Engineering Mechanics 58 (2019) 103001

Contents lists available at ScienceDirect

Probabilistic Engineering Mechanics

journal homepage: www.elsevier.com/locate/probengmech

Reliability analysis of nonlinear dynamic system with epistemic uncertainties using hybrid Kriging-HDMR

Dawei Li [a], Hesheng Tang [a,b,*], Songtao Xue [a], Xueyuan Guo [a]

[a] Department of Disaster Mitigation for Structures, College of Civil Engineering, Tongji University, 1239 Siping Rd., Shanghai 200092, China
[b] State Key Laboratory of Disaster Reduction in Civil Engineering, Tongji University, 1239 Siping Rd., Shanghai 200092, China

ARTICLE INFO

Keywords:
Epistemic uncertainty
First passage probability
Interval model
Hybrid Kriging-HDMR
Differential evolution

ABSTRACT

The small first passage probability of nonlinear dynamic structures under nonstationary seismic excitation implies a prohibitive computational demand because of the epistemic uncertainties rooted in structure system. In this work, a hybrid Kriging-high dimensional model representation (Kriging-HDMR) methodology for drastically simplifying this task is proposed. The epistemic uncertainties with well-defined bounds but no concrete distribution forms are addressed by interval model. Therefore, the first passage probability of the generic response process that the epistemic uncertainties involved, is represented by the conditional univariate extreme value distribution (EVD) of structural parameters with interval form. Then, a Kriging assisted HDMR together with third moment saddle point approximation (TMSA) is proposed to alleviate the computational burden and provides an accurate depiction of possible model outcome. The differential evolution (DE) interval optimization strategy is performed to accelerate the post process of searching the lower bound (LB) and upper bound (UB) of first passage probability with interval form. Finally, a nine-story shear frame with Bouc–Wen model is presented to demonstrate the accuracy and efficiency of proposed method.

1. Introduction

The first passage probability is of paramount importance in structural engineering that delivers the ability to satisfy several performance requirements within a specified time span. During the past few decades, such an extensive effort has been devoted in this topic. On the basis of well-established stochastic process and probability theorem, the randomness of outside excitation was firstly considered and the substantial achievements are obtained, such as, mean out-crossing based formulation [1] and its extensions [2–4] were proposed to evaluate the first passage probability of linear structure under stationary or nonstationary excitation. As one might expect, the analytical solution of mean out-crossing may seldom amendable for nonlinear system due to its theoretical background [5]. On the other hand, the simulation-based methods may overcome this dilemma. This measure is beginning by Shinozuka [6,7], who combined the power spectral representation and Monte-Carlo (MC) simulation to model the stochastic excitation in stochastic dynamic analysis. While, substantial amounts of samples of brute force simulations requires significant computational and analysis time for large and complex systems. To overcome this problem, the importance simulation [8], subset simulation method [9] and MC-based extreme value distribution [10] are developed. Some other potential approximation methods, such as equivalent linearization method [11], trail equivalent linearization method [12], generalized extreme value distribution [13], generalized Gaussian distribution [14], shifted generalized lognormal distribution [15,16], kernel density maximum entropy [17], are also developed in prediction of first passage probability.

However, not only the outside excited loads demonstrate uncertain, but also structural systems. Apart from the randomness of excited loads, the uncertainties of structural systems are always epistemic due to incomplete information, ignorance, or modeling (e.g., simplification of mathematical models of buildings for structural analysis) [18]. As the classical methodology, the uncertainties of structural system are seemed as randomness. Zhang and co-workers [19] developed a fourth-statistical moments based Edgeworth series expansion to approximate the first passage for single degree-of-freedom nonlinear oscillators with random parameters. Chaudhuri et al. [20] presented a perturbation based conditional first passage probability with uncertain parameters. Gupta [21] proposed a first order Taylor expansion based analytical framework for first passage probability analysis of vibrating structures with random parameters. Sundar et al. [22] combined Girsanov transformation and subset simulation to investigate the benchmark problem [23]. However, the extremely insufficient data may lead to an ambiguous form of probability distribution. Furthermore, Refs. [24,25] demonstrated that a tiny fluctuation of probability model would lead a large bias of reliability approximation. From another aspect,

* Corresponding author.
E-mail address: thstj@tongji.edu.cn (H. Tang).

https://doi.org/10.1016/j.probengmech.2019.103001
Received 12 October 2018; Received in revised form 7 June 2019; Accepted 12 September 2019
Available online 19 September 2019

the probability theory gives an excessively optimistic quantification result but cannot sufficiently emphasize extremes or epistemic uncertainties. Alternatively, the non-probability theories are applicable to model imprecise, vague, fuzzy, and incomplete variabilities involved in engineering. Among the potential non-probability theories [26–28], interval theory is more perfect to model the uncertainties that the lower and upper bounds are well defined but the concrete distribution form is missing. The interval theory was initialized by Moore [27] and has been implemented in static response analysis of structures [29], time variant excitation [30]. To the best of the authors' knowledge, the endeavors of interval theory addressed in first passage probability approximation are limited. Muscolino etc. [31–33] proposed an interval based up-crossings rate formulation of linear structures under Gaussian random process. Do and co-workers [34] employed an improved particle swarm optimization algorithm to search the lower and upper bounds of dynamic reliability for an interval based structural system. Wang et al. [35,36]successfully implemented the interval and convex model to investigate the influence of the independent and dependent epistemic uncertainties in time variant reliability analysis.

Although some attempts have been implemented in linear system response, there are still latent challenges regarding the first passage probability of nonlinear system with interval uncertainties. One of major challenges of this topic is the formulation of first passage probability with interval uncertainties rooted in structural system. In this framework, the approximation of interval first passage probability is equivalent to estimate the lower bound (LB) and upper bound (UB) of an extreme value distribution (EVD) with a specified threshold value [13,37]. However, the evaluation of LB and UB of EVD may be trapped in the high dimensional uncertainty quantification problem, often known as the"curse of dimensionality". To overcome this deficiency, the high dimensional model representation (HDMR) is presented to reduce the computational cost for high dimensional problem. The HDMR is an efficient meta-model for high dimensional mapping for large and complex system with weak correlations of higher order variable, which reflected in most physical model [38]. With the evidential character for dramatically reducing the computational dimensions, HDMRs are developed and applied for various purposes [39–41]. In this work, a combination of HDMR and Kriging interpolation technique [42] is presented to construct the meta-model of first passage probability of nonlinear system with interval uncertainties. The realization of Kriging model is approximated by the third moment saddle point approximation (TMSA) [43]. After construction of meta-model, the differential evolution (DE) interval optimization technique [44] is presented to search the LB and UB of interval formed first passage probability.

The remaining parts of this paper are organized as follows. Section 2 provides the formulation of dynamic reliability considering the uncertainty of structural parameters. Section 3 explains interval modeling of dynamic reliability with interval numbers. Section 4 describes the HDMR combining Kriging interpolation and TMSA methodology. Section 5 gives the DE based evaluation method for LB and UB of interval formed first passage probability. A 9-story shear frame with Bouc–Wen model is presented in Section 6 to investigate the effectiveness and accuracy of the proposed method. Based on the studies in this work, some conclusions are drawn in Section 7.

2. Dynamic reliability with uncertain structural parameters

Without loss of the generality, a mathematical expression of dynamic system is simplified as:

$$\mathbf{M}(\boldsymbol{\theta})\ddot{\mathbf{X}}\left(\boldsymbol{\theta},\boldsymbol{\eta},t\right)+\mathbf{C}(\boldsymbol{\theta})\dot{\mathbf{X}}\left(\boldsymbol{\theta},\boldsymbol{\eta},t\right)+\mathbf{R}(\boldsymbol{\theta},\boldsymbol{\eta},t)=\mathbf{F}(\boldsymbol{\theta},\boldsymbol{\eta},t) \tag{1}$$

where $\ddot{\mathbf{X}}\left(\boldsymbol{\theta},\boldsymbol{\eta},t\right)$ and $\dot{\mathbf{X}}\left(\boldsymbol{\theta},\boldsymbol{\eta},t\right)$ denote the $n\times1$ acceleration and velocity vectors, respectively; $\mathbf{M}(\boldsymbol{\theta})$ and $\mathbf{C}\left(\boldsymbol{\theta}\right)$ denote the $n\times n$ mass and damping matrices, respectively; $\mathbf{R}\left(\boldsymbol{\theta},\boldsymbol{\eta},t\right)$ is the $n\times1$ restoring force vector. The symbol $\boldsymbol{\theta}=[\theta_1,\theta_2,\ldots,\theta_d]^{\mathrm{T}}$ is a d-dimensional uncertain vector involving structural parameters with epistemic uncertainties; $\boldsymbol{\eta}=[\eta_1,\eta_2,\ldots,\eta_m]^{\mathrm{T}}$ is a m-dimensional uncertain vector that is used to represent the uncertainties rooted in outside excitation; $\mathbf{F}(\boldsymbol{\theta},\boldsymbol{\eta},t)$ denotes the $n\times1$ output excitation vector. For a well posed dynamic system, the system response quantities of interest $\mathbf{Z}(\boldsymbol{\theta},\boldsymbol{\eta},t)$ is expressed as:

$$\mathbf{Z}\left(\boldsymbol{\theta},\boldsymbol{\eta},t\right)=\mathrm{H}\left(\ddot{\mathbf{X}}\left(\boldsymbol{\theta},\boldsymbol{\eta},t\right),\dot{\mathbf{X}}\left(\boldsymbol{\theta},\boldsymbol{\eta},t\right),\mathbf{X}\left(\boldsymbol{\theta},\boldsymbol{\eta},t\right)\right) \tag{2}$$

where $\mathbf{Z}(\boldsymbol{\theta},\boldsymbol{\eta},t)$ is $L\times1$ observation quantities of structural states. Given a series of threshold values $b_\tau,b_1<\cdots,<b_\tau<,\ldots,<b_\Gamma$, the failure probability of dynamic system response at time cut t_i with different threshold value b_τ is defined as:

$$P_f\left(\boldsymbol{\theta},\boldsymbol{\eta},b_\tau,t_i\right)=P\left\{\bigcup_{l=1}^{L}Z_l\left(\boldsymbol{\theta},\boldsymbol{\eta},t_i\right)\geq b_\tau,\exists t_i\in[0,T]\right\} \tag{3}$$

The equivalent expression of Eq. (3) can be expressed as:

$$\begin{aligned}&P\left\{\bigcup_{l=1}^{L}Z_l\left(\boldsymbol{\theta},\boldsymbol{\eta},t_i\right)\geq b_\tau,\exists t_i\in[0,T]\right\}\\&=1-P\left\{\bigcap_{l=1}^{L}Z_l\left(\boldsymbol{\theta},\boldsymbol{\eta},t_i\right)\leq b_\tau,\exists t_i\in[0,T]\right\}\end{aligned} \tag{4}$$

As defined in Refs. [16,21,37], suppose $Z_1\left(\boldsymbol{\theta},\boldsymbol{\eta},t_i\right),\ldots,Z_l\left(\boldsymbol{\theta},\boldsymbol{\eta},t_i\right),\ldots,Z_L\left(\boldsymbol{\theta},\boldsymbol{\eta},t_i\right)$ are random variables and let $Z_{\mathrm{ext}}\left(\boldsymbol{\theta},\boldsymbol{\eta},t_i\right)=\max_{l\in[1,L]}\left\{Z_l\left(\boldsymbol{\theta},\boldsymbol{\eta},t_i\right)\right\}$, the right hands of Eq. (4) are rewritten as:

$$\begin{aligned}&P\left\{Z_{\mathrm{ext}}\left(\boldsymbol{\theta},t_i\right)\leq b_\tau,\exists t_i\in[0,T]\right\}\\&=P\left\{\bigcap_{l=1}^{L}Z_l\left(\boldsymbol{\theta},\boldsymbol{\eta},t_i\right)\leq b_\tau,\exists t_i\in[0,T]\right\}\end{aligned} \tag{5}$$

Define $\tilde{Z}_{\mathrm{ext}}\left(\boldsymbol{\theta},\boldsymbol{\eta},T\right)=\max_{t_i\in[0,T]}\left\{Z_{\mathrm{ext}}\left(\boldsymbol{\theta},\boldsymbol{\eta},t_i\right)\right\}$, the corresponding extreme value distribution (EVD) of $\mathbf{Z}(\boldsymbol{\theta},\boldsymbol{\eta},t)$ in time interval $[0,T]$ is defined as:

$$P\left\{\widetilde{Z}_{\mathrm{ext}}\left(\boldsymbol{\theta},\boldsymbol{\eta},T\right)\leq b_\tau\right\}=P\left\{\bigcap_{i=1}^{N}Z_{\mathrm{ext}}\left(\boldsymbol{\theta},\boldsymbol{\eta},t_i\right)\leq b_\tau\right\} \tag{6}$$

Then, the first passage probability of dynamic response of structural system is expressed as:

$$P_f\left(\boldsymbol{\theta},\boldsymbol{\eta},b_\tau,T\right)=1-P\left\{\widetilde{Z}_{\mathrm{ext}}\left(\boldsymbol{\theta},\boldsymbol{\eta},T\right)\leq b_\tau\right\} \tag{7}$$

where,

$$P\left\{\widetilde{Z}_{\mathrm{ext}}\left(\boldsymbol{\theta},\boldsymbol{\eta},T\right)\leq b_\tau\right\}=P\left\{\bigcap_{i=1}^{N}\bigcap_{l=1}^{L}Z_l\left(\boldsymbol{\theta},\boldsymbol{\eta},t_i\right)\leq b_\tau\right\} \tag{8}$$

To obtain the computational results of first passage probability, the total probability theorem (TPT), the $P\left\{\tilde{Z}_{\mathrm{ext}}\left(\boldsymbol{\theta},\boldsymbol{\eta},T\right)\leq b_\tau\right\}$ is expressed with the continuous form:

$$\begin{aligned}&P\left\{\widetilde{Z}_{\mathrm{ext}}\left(\boldsymbol{\theta},\boldsymbol{\eta},T\right)\leq b_\tau\right\}\\&=\int_{\Omega_{\boldsymbol{\eta}}}\int_{\Omega_{\boldsymbol{\theta}}}p\left\{\widetilde{Z}_{\mathrm{ext}}\left(\boldsymbol{\theta},\boldsymbol{\eta},T\right)\leq b_\tau\left|\boldsymbol{\theta}=\boldsymbol{\theta}^0\right.\right\}p\left(\boldsymbol{\theta}^0\right)\mathrm{d}\boldsymbol{\eta}\mathrm{d}\boldsymbol{\theta}^0,\ \boldsymbol{\theta}^0\in\Omega_{\boldsymbol{\theta}}\end{aligned} \tag{9}$$

or with discrete form:

$$\begin{aligned}&P\left\{\widetilde{Z}_{\mathrm{ext}}\left(\boldsymbol{\theta},\boldsymbol{\eta},T\right)\leq b_\tau\right\}\\&=\sum_{i=1}^{N}P\left(\boldsymbol{\theta}_i^0\right)\int_{\Omega_{\boldsymbol{\eta}}}p\left\{\widetilde{Z}_{\mathrm{ext}}\left(\boldsymbol{\theta},\boldsymbol{\eta},T\right)\leq b_\tau\left|\boldsymbol{\theta}=\boldsymbol{\theta}_i^0\right.\right\}\mathrm{d}\boldsymbol{\eta},\ \boldsymbol{\theta}_i^0\in\Omega_{\boldsymbol{\theta}}\end{aligned} \tag{10}$$

where, the continuous form $p\left\{\tilde{Z}_{\mathrm{ext}}\left(\boldsymbol{\theta},\boldsymbol{\eta},T\right)\leq b_\tau|\boldsymbol{\theta}=\boldsymbol{\theta}^0\right\}$ or discrete form $P\left\{\tilde{Z}_{\mathrm{ext}}\left(\boldsymbol{\theta},\boldsymbol{\eta},T\right)\leq b_\tau|\boldsymbol{\theta}=\boldsymbol{\theta}_i^0\right\}$ denote the conditional probability of first passage probability of dynamic system response; $p\left(\boldsymbol{\theta}^0\right)$ or $P\left(\boldsymbol{\theta}_i^0\right)$ denote the joint probability density function (PDF) in Eq. (9) or joint probability mass function in Eq. (10) of the input variable $\boldsymbol{\theta}$; $\boldsymbol{\Omega}_{\boldsymbol{\theta}}$ denotes the support field of $p\left(\boldsymbol{\theta}^0\right)$ or $P\left(\boldsymbol{\theta}_i^0\right)$; N denotes the number of support point in $\boldsymbol{\Omega}_{\boldsymbol{\theta}}$; and the $\boldsymbol{\Omega}_{\boldsymbol{\eta}}$ is the support domain of outside excitation uncertainties $\boldsymbol{\eta}$. As shown in above theoretical deviations, the expression of dynamic reliability of structural system is obtained. However, it should be noted that the essence of probabilistic

distribution may not sufficiently address the complex mechanics and scarce information of structural uncertainties $\boldsymbol{\theta}$. From another side, the boundary range of uncertain variable is suitable to describe the epistemic uncertainty $\boldsymbol{\theta}$ that always demonstrate the fluctuation around its nominal value. Integrating the information provided so far, the interval model is presented to investigate the dynamic reliability with epistemic uncertainties with the well-defined bounds but not concrete distribution form.

3. Interval modeling of dynamic reliability with epistemic uncertainties

The interval numbers theory is originally proposed by Moore [27] to descript the uncertainty form limit data and lack of knowledge. Given a vector of uncertain parameter $\boldsymbol{\theta} = [\theta_1, \theta_2, \ldots, \theta_d]^{\mathrm{T}}$, the interval representation of $\boldsymbol{\theta}$ is defined as $\boldsymbol{\theta}^{\mathrm{I}} = [\theta_1^{\mathrm{I}}, \theta_2^{\mathrm{I}}, \ldots, \theta_d^{\mathrm{I}}]^{\mathrm{T}}$. According to interval representation rule, the bounds of interval parameters vector can be written as:

$$\boldsymbol{\theta}^{\mathrm{I}} = \left(\theta_i^{\mathrm{I}}\right) = \left[\boldsymbol{\theta}^{\mathrm{med}} - \boldsymbol{\theta}^{\mathrm{rad}}, \boldsymbol{\theta}^{\mathrm{med}} + \boldsymbol{\theta}^{\mathrm{rad}}\right] \tag{11}$$

in which,

$$\begin{aligned} &\boldsymbol{\theta}^{\mathrm{med}} = \left(\theta_i^{\mathrm{med}}\right) = \left(\underline{\boldsymbol{\theta}} + \overline{\boldsymbol{\theta}}\right)/2, \\ &\boldsymbol{\theta}^{\mathrm{rad}} = \left(\theta_i^{\mathrm{rad}}\right) = \left(\overline{\boldsymbol{\theta}} - \underline{\boldsymbol{\theta}}\right)/2, \ i = 1, 2, \ldots, d \end{aligned} \tag{12}$$

where, the symbol $\boldsymbol{\theta}^{\mathrm{med}}$ and $\boldsymbol{\theta}^{\mathrm{rad}}$ denote the midpoint and radius of $\underline{\boldsymbol{\theta}}$; and $\overline{\boldsymbol{\theta}}$ denotes the LB and UB of interval $\boldsymbol{\theta}$. The fluctuation of an interval variable is defined as the degree of uncertain level v_i:

$$v_i = \theta_i^{\mathrm{rad}}/\theta_i^{\mathrm{med}} \tag{13}$$

Taking the interval uncertainties $\boldsymbol{\theta}$ into Eq. (10), the value of EVD $P\left\{\tilde{Z}_{\mathrm{ext}}\left(\boldsymbol{\theta}, \boldsymbol{\eta}, T\right) \le b_\tau | \boldsymbol{\theta} = \boldsymbol{\theta}_i^0\right\}$ and first passage probability $P_f\left(\boldsymbol{\theta}, \boldsymbol{\eta}, b_\tau, T\right)$ becomes an interval:

$$\begin{aligned} &\left[\underline{P}_f\left(\boldsymbol{\theta}^{\mathrm{I}}, \boldsymbol{\eta}, b_\tau, T\right), \overline{P}_f\left(\boldsymbol{\theta}^{\mathrm{I}}, \boldsymbol{\eta}, b_\tau, T\right)\right] \\ &= \left[1 - \overline{P}\left\{\widetilde{Z}_{\mathrm{ext}}\left(\boldsymbol{\theta}, \boldsymbol{\eta}, T\right) \le b_\tau \middle| \boldsymbol{\theta} = \boldsymbol{\theta}^{\mathrm{I}}\right\}, \right. \\ &\qquad \left. 1 - \underline{P}\left\{\widetilde{Z}_{\mathrm{ext}}\left(\boldsymbol{\theta}, \boldsymbol{\eta}, T\right) \le b_\tau \middle| \boldsymbol{\theta} = \boldsymbol{\theta}^{\mathrm{I}}\right\}\right] \end{aligned} \tag{14}$$

where,

$$\begin{aligned} &\overline{P}\left\{\widetilde{Z}_{\mathrm{ext}}\left(\boldsymbol{\theta}, \boldsymbol{\eta}, T\right) \le b_\tau | \boldsymbol{\theta} = \boldsymbol{\theta}^{\mathrm{I}}\right\} \\ &= \underset{\boldsymbol{\theta}_{\mathrm{temp}} \in \boldsymbol{\theta}^{\mathrm{I}}}{\mathrm{maximize}} \left\{\int_{\boldsymbol{\Omega}_{\boldsymbol{\eta}}} p\left\{\widetilde{Z}_{\mathrm{ext}}\left(\boldsymbol{\theta}, \boldsymbol{\eta}, T\right) \le b_\tau \middle| \boldsymbol{\theta} = \boldsymbol{\theta}_{\mathrm{temp}}\right\} \mathrm{d}\boldsymbol{\eta}\right\}, \end{aligned} \tag{15}$$

$$\begin{aligned} &\underline{P}\left\{\widetilde{Z}_{\mathrm{ext}}\left(\boldsymbol{\theta}, \boldsymbol{\eta}, T\right) \le b_\tau | \boldsymbol{\theta} = \boldsymbol{\theta}^{\mathrm{I}}\right\} \\ &= \underset{\boldsymbol{\theta}_{\mathrm{temp}} \in \boldsymbol{\theta}^{\mathrm{I}}}{\mathrm{minimize}} \left\{\int_{\boldsymbol{\Omega}_{\boldsymbol{\eta}}} p\left\{\widetilde{Z}_{\mathrm{ext}}\left(\boldsymbol{\theta}, \boldsymbol{\eta}, T\right) \le b_\tau \middle| \boldsymbol{\theta} = \boldsymbol{\theta}_{\mathrm{temp}}\right\} \mathrm{d}\boldsymbol{\eta}\right\}, \end{aligned} \tag{16}$$

As shown in Eqs. (14)–(16), the estimation of LB and UB of first passage probability involves a nested-loop solution procedure, in which, the inner loop manages treatment of aleatory uncertainties and outer loop affords treatment of epistemic uncertainties. Strictly speaking, the nested-loop Monte-Carlo (MC) method can afford the most accurate solutions, as shown in Eqs. (15)–(16). Unfortunately, the approximation of inner integration $\int_{\Omega_{\boldsymbol{\eta}}} p\{\tilde{Z}_{\mathrm{ext}}(\boldsymbol{\theta}, \boldsymbol{\eta}, T) \le b_\tau | \boldsymbol{\theta} = \boldsymbol{\theta}_{\mathrm{temp}}\}$ always involves hundreds even thousands of variables may lead to tremendous computational challenges for nested-loop MC simulation. On the other hand, the outer-loop solution procedure needs such a large number of samples to determine the maximum and minimum value corresponding to interval variables. To overcome the inefficiency of nested-loop MC, meta-model that combines third moment saddle point approximation (TMSA) and high dimensional model representation (HDMR) technique is employed in this work to replace the high dimensional integration $\int_{\Omega_{\boldsymbol{\eta}}} p\{\tilde{Z}_{\mathrm{ext}}(\boldsymbol{\theta}, \boldsymbol{\eta}, T) \le b_\tau | \boldsymbol{\theta} = \boldsymbol{\theta}_{\mathrm{temp}}\}$ and decrease the computational burden. In our proposed method, the TMSA-HDMR will be adopted as meta-model to predict the interval extreme value probability response of $P\{\tilde{Z}_{\mathrm{ext}}(\boldsymbol{\theta}, \boldsymbol{\eta}, T) \le b_\tau | \boldsymbol{\theta} = \boldsymbol{\theta}_{\mathrm{temp}}\}$. Then, the evaluation of LB and UB of first passage probability are converted to the searching minimum and maximum values of constructed HDMR in the epistemic variable space $\left[\underline{\boldsymbol{\theta}}, \overline{\boldsymbol{\theta}}\right]$.

4. Meta-model for the evaluation of EVD

In line with the derivations of Section 3, the approximation of LB and UB of first passage probability is transformed as the evaluation of the bounds of $P\{\tilde{Z}_{\mathrm{ext}}(\boldsymbol{\theta}, \boldsymbol{\eta}, T) \le b_\tau | \boldsymbol{\theta} = \boldsymbol{\theta}^{\mathrm{I}}\}$ with an interval vector $\boldsymbol{\theta}^{\mathrm{I}}$. In this section, the detailed information of meta-model is presented. HDMR is the mapping hierarchical relationship between the d-dimensional system input $\mathbf{x} = \left[x_1, x_2, \ldots, x_d\right]^{\mathrm{T}}$ and a continuous, differentiable, real-valued, m-dimensional system response $f(\mathbf{x})$.

$$f(\mathbf{x}) = f^0 + \sum_{i=1}^{d} f^1\left(x_i\right) + \sum_{1 \le i \le j \le d} f^2\left(x_i, x_j\right) + \cdots, + f^d\left(x_1, x_2, \ldots, x_d\right) \tag{17}$$

where f^0 is the constant term of denoting the zeroth-order effect of system input. The $f^1\left(x_i\right)$ is the first-order term of the expansion of $f(\mathbf{x})$ denoting the individual contribution of univariate x_i to the system response $f(\mathbf{x})$. The $f^2\left(x_i, x_j\right)$ is the second-order term of expansion of $f(\boldsymbol{x})$ denoting the cooperative effect of bivariate x_i and x_j to the system response $f(\mathbf{x})$. The last term $f^d\left(x_1, x_2, \ldots, x_d\right)$ is the dth-order cooperative effect of $x_1, x_2, \ldots, x_d$, denoting the residual dependence of all input variables together to effect the system response $f(\mathbf{x})$. As documented the basis of HDMR in [45], the target function is accurately represented by the sum of D expansion terms, where $D = \sum_{i=0}^{d} d!(d-i)!/i!$. However, it should be noted that the most physical systems always manifest the effect hierarchy principle [38,45], lower-order effects are more important than higher order effects. In other words, the lower expansion of HDMR would be adequate to describe the practical system behavior. In this context, the second order expansion of HDMR is used to construct the meta-model of the mapping between epistemic uncertainties in structural system. Using the second order HDMR, the approximation of $P\{\tilde{Z}_{\mathrm{ext}}(\boldsymbol{\theta}, \boldsymbol{\eta}, T) \le b_\tau | \boldsymbol{\theta} = \boldsymbol{\theta}_{\mathrm{temp}}\}$ is rewritten as:

$$\begin{aligned} &P\left\{\widetilde{Z}_{\mathrm{ext}}\left(\boldsymbol{\theta}, \boldsymbol{\eta}, T\right) \le b_\tau \middle| \boldsymbol{\theta} = \boldsymbol{\theta}_{\mathrm{temp}}\right\} \\ &= \begin{pmatrix} \sum_{1 \le i \le j \le d} P^2\left\{\widetilde{Z}_{\mathrm{ext}}\left(\boldsymbol{\theta}_{i,j}^2, \boldsymbol{\eta}, T\right) \le b_\tau\right\} \\ -(d-1)\sum_{i=1}^{d} P^1\left\{\widetilde{Z}_{\mathrm{ext}}\left(\boldsymbol{\theta}_i^1, \boldsymbol{\eta}, T\right) \le b_\tau\right\} \\ +\frac{(d-1)(d-2)}{2} P^0\left\{\widetilde{Z}_{\mathrm{ext}}\left(\boldsymbol{\theta}^0, \boldsymbol{\eta}, T\right) \le b_\tau\right\} \end{pmatrix} + \varepsilon \end{aligned} \tag{18}$$

where,

$$\begin{aligned} P^2\left\{\widetilde{Z}_{\mathrm{ext}}\left(\boldsymbol{\theta}_{i,j}^2, \boldsymbol{\eta}, T\right) \le b_\tau\right\} &= \int_{\boldsymbol{\Omega}_{\boldsymbol{\eta}}} p\left\{\widetilde{Z}_{\mathrm{ext}}\left(\boldsymbol{\theta}_{i,j}^2, \boldsymbol{\eta}, T\right) \le b_\tau \middle| \boldsymbol{\theta}_{i,j}^2 \right. \\ &\left. = \left[\theta_1^0, \ldots, \theta_i, \ldots, \theta_j, \ldots, \theta_d^0\right]^{\mathrm{T}}\right\} \mathrm{d}\boldsymbol{\eta} \end{aligned} \tag{19}$$

$$\begin{aligned} P^1\left\{\widetilde{Z}_{\mathrm{ext}}\left(\boldsymbol{\theta}_i^1, \boldsymbol{\eta}, T\right) \le b_\tau\right\} &= \int_{\boldsymbol{\Omega}_{\boldsymbol{\eta}}} p\left\{\widetilde{Z}_{\mathrm{ext}}\left(\boldsymbol{\theta}_i^1, \boldsymbol{\eta}, T\right) \le b_\tau \middle| \boldsymbol{\theta}_i^1 \right. \\ &\left. = \left[\theta_1^0, \ldots, \theta_i, \ldots, \theta_d^0\right]^{\mathrm{T}}\right\} \mathrm{d}\boldsymbol{\eta} \end{aligned} \tag{20}$$

$$\begin{aligned} P^0\left\{\widetilde{Z}_{\mathrm{ext}}\left(\boldsymbol{\theta}^0, \boldsymbol{\eta}, T\right) \le b_\tau\right\} &= \int_{\boldsymbol{\Omega}_{\boldsymbol{\eta}}} p\left\{\widetilde{Z}_{\mathrm{ext}}\left(\boldsymbol{\theta}^0, \boldsymbol{\eta}, T\right) \le b_\tau \middle| \boldsymbol{\theta}^0 \right. \\ &\left. = \left[\theta_1^0, \ldots, \theta_i^0, \ldots, \theta_d^0\right]^{\mathrm{T}}\right\} \mathrm{d}\boldsymbol{\eta} \end{aligned} \tag{21}$$

where, $\boldsymbol{\theta}_{\mathrm{temp}} = \left(\theta_1, \ldots, \theta_i, \ldots, \theta_j, \ldots, \theta_d\right)$ denotes the interesting point to be computed; $\boldsymbol{\theta}^0 = \left(\theta_1^0, \theta_2^0, \ldots, \theta_d^0\right)$ denotes the origin of variable space $\mathbf{V}(\boldsymbol{\theta}) = \left[\underline{\theta_1}, \overline{\theta_1}\right] \times \left[\underline{\theta_2}, \overline{\theta_2}\right] \times, \ldots, \times \left[\underline{\theta_d}, \overline{\theta_d}\right]$ and the symbol ε denotes the residual error for the HDMR. According to the definitions of interval number theory, the constant term $P^0\{\tilde{Z}_{\mathrm{ext}}(\boldsymbol{\theta}^0, \boldsymbol{\eta}, T) \le b_\tau\}$ is computed by fixed the variable input at support point $\boldsymbol{\theta}^{\mathrm{med}} =$

$\left(\theta_1^{\text{med}}, \theta_2^{\text{med}}, \ldots, \theta_d^{\text{med}}\right)$. The first order term $P^1\{\tilde{Z}_{\text{ext}}(\boldsymbol{\theta}_i^1, \boldsymbol{\eta}, T) \le b_\tau\}$ is the response of $P\{\tilde{Z}_{\text{ext}}(\boldsymbol{\theta}, \boldsymbol{\eta}, T) \le b_\tau\}$at cut line $\boldsymbol{\theta}_i^1 = \left(\theta_1^{\text{med}}, \ldots, \theta_i, \ldots, \theta_d^{\text{med}}\right)$. The second order terms $P^2\{\tilde{Z}_{\text{ext}}(\boldsymbol{\theta}_{i,j}^2, \boldsymbol{\eta}, T) \le b_\tau\}$ is the response of $P\{\tilde{Z}_{\text{ext}}(\boldsymbol{\theta}, \boldsymbol{\eta}, T) \le b_\tau\}$at cut plane $\boldsymbol{\theta}_{i,j}^2 = \left(\theta_1^{\text{med}}, \ldots, \theta_i, \ldots, \theta_j, \ldots, \theta_d^{\text{med}}\right)$. As reflected in Eq. (18), $P\{\tilde{Z}_{\text{ext}}(\boldsymbol{\theta}, \boldsymbol{\eta}, T) \le b_\tau | \boldsymbol{\theta} = \boldsymbol{\theta}_{\text{temp}}\}$ is represented by the combination of the zeroth, first order and second order terms. Similar to other meta-models, the most crucial step of construction of HDMR is determination of the sub-expression of expansion terms. Because the implicit formulation of high dimensional integration $\int_{\Omega_{\boldsymbol{\eta}}} p\{\tilde{Z}_{\text{ext}}(\boldsymbol{\theta}, \boldsymbol{\eta}, T) \le b_\tau | \boldsymbol{\theta} = \boldsymbol{\theta}_{\text{temp}}\}$, it is hard to construct an explicit formulation of first-order and second-order terms of HDMR. To improve the computational efficiency and accuracy, a wise choice is to use the sub-level surrogate model to replace the complicated time history analysis. Herein, the classical kriging model is used to approximate the response of univariate function $P^1\{\tilde{Z}_{\text{ext}}(\boldsymbol{\theta}_i^1, \boldsymbol{\eta}, T) \le b_\tau\}$ and bivariate function $P^2\{\tilde{Z}_{\text{ext}}(\boldsymbol{\theta}_{i,j}^2, \boldsymbol{\eta}, T) \le b_\tau\}$.

4.1. Kriging HDMR based conditional meta-model of epistemic uncertainty

The DACE toolbox [42] is employed in this work to build the lower-order terms of HDMR. This section briefly summary the principle of Kriging, a more detailed introduction of is presented in [42,46]. In Kriging model, the system response $\mathbf{y}(\mathbf{x})$ is represented as:

$$\mathbf{y}(\mathbf{x}) = \mathbf{g}^{\mathrm{T}}(\mathbf{x})\boldsymbol{\beta} + z(\mathbf{x}) \tag{22}$$

in which, $\mathbf{g}^{\mathrm{T}}(\mathbf{x})\boldsymbol{\beta}$ gives the trend term of Kriging. The $\mathbf{g}(\mathbf{x}) = \left[g_1(\mathbf{x}), g_2(\mathbf{x}), \ldots, g_k(\mathbf{x})\right]^{\mathrm{T}}$ is the vector of basis functions and $\boldsymbol{\beta} = \left[\beta_1, \beta_2, \ldots, \beta_k\right]^{\mathrm{T}}$ is the vector of regression coefficients. The residual process $z(\mathbf{x})$ is defined with zero mean and the following covariance between two points:

$$\mathrm{Cov}\left(z(x), z\left(\tilde{x}\right)\right) = \sigma^2 R\left(\omega, x, \tilde{x}\right) \tag{23}$$

where σ^2 is the stochastic process variance, $R(\omega, x, \tilde{x})$ is the correlation function of x and $\tilde{x}$ with parameter ω. Given a design set $\mathbf{X}_{\mathrm{D}} = \left\{\mathbf{x}_1, \mathbf{x}_2, \ldots, \mathbf{x}_m\right\}$ and corresponding system response set $\mathbf{Y}_{\mathrm{D}} = \left\{y(\mathbf{x}_1), y(\mathbf{x}_1), \ldots, y(\mathbf{x}_m)\right\}$, the parameter ω is determined by using maximum likelihood estimation. With an optimal parameter ω, the value of $R(\omega, x, \tilde{x})$ is determined, thus the prediction of sample is determined as:

$$\hat{y}(\mathbf{x}) = \mathbf{g}^{\mathrm{T}}\boldsymbol{\beta} + \mathbf{r}^{\mathrm{T}}\mathbf{R}^{-1}\left(\mathbf{Y}_{\mathrm{D}} - \mathbf{G}^{\mathrm{T}}\boldsymbol{\beta}\right) \tag{24}$$

in which, $\boldsymbol{\beta} = \left(\mathbf{G}^{\mathrm{T}}\mathbf{R}^{-1}\mathbf{G}\right)^{-1}\mathbf{G}^{\mathrm{T}}\mathbf{R}^{-1}\mathbf{Y}_{\mathrm{D}}$, $\mathbf{G} = \left\{\mathbf{g}(\mathbf{x}_1), \mathbf{g}(\mathbf{x}_2), \ldots, \mathbf{g}(\mathbf{x}_m)\right\}$. In this work, we set the basis function $\mathbf{g}(\mathbf{x}) = 1$, then the $\boldsymbol{\beta}$ becomes a scalar β. The first-order term $P^1\{\tilde{Z}_{\text{ext}}(\boldsymbol{\theta}_i^1, \boldsymbol{\eta}, T) \le b_\tau\}$ and second-order term $P^2\{\tilde{Z}_{\text{ext}}(\boldsymbol{\theta}_{i,j}^2, \boldsymbol{\eta}, T) \le b_\tau\}$ are constructed by Kriging model as shown in Eqs. (25)–(26):

$$\hat{P}^1\left\{\widetilde{Z}_{\text{ext}}\left(\boldsymbol{\theta}_i^1, \boldsymbol{\eta}, T\right) \le b_\tau\right\} = \beta_1 + \mathbf{r}_i^{\mathrm{T}}\left(\boldsymbol{\theta}_i^1\right)\mathbf{R}_i^{-1}\left(\mathbf{Y}_{\mathrm{D}}^1 - \mathbf{1}^{\mathrm{T}}\beta_1\right) \tag{25}$$

$$\hat{P}^2\left\{\widetilde{Z}_{\text{ext}}\left(\boldsymbol{\theta}_{ij}^2, \boldsymbol{\eta}, T\right) \le b_\tau\right\} = \beta_2 + \mathbf{r}_{ij}^{\mathrm{T}}\left(\boldsymbol{\theta}_{ij}^2\right)\mathbf{R}_{ij}^{-1}\left(\mathbf{Y}_{\mathrm{D}}^2 - \mathbf{1}^{\mathrm{T}}\beta_2\right) \tag{26}$$

where, $\beta_1 = \left(\mathbf{1}^{\mathrm{T}}\mathbf{R}^{-1}\mathbf{1}\right)^{-1}\mathbf{1}^{\mathrm{T}}\mathbf{R}_i^{-1}\mathbf{Y}_{\mathrm{D}}^1$, $\beta_2 = \left(\mathbf{1}^{\mathrm{T}}\mathbf{R}^{-1}\mathbf{1}\right)^{-1}\mathbf{1}^{\mathrm{T}}\mathbf{R}_{ij}^{-1}\mathbf{Y}_{\mathrm{D}}^2$ are used to represented the regression coefficient for $\hat{P}^1\{\tilde{Z}_{\text{ext}}(\boldsymbol{\theta}_i^1, \boldsymbol{\eta}, T) \le b_\tau\}$ and $\hat{P}^2\{\tilde{Z}_{\text{ext}}(\boldsymbol{\theta}_{i,j}^2, \boldsymbol{\eta}, T) \le b_\tau\}$, respectively. The Gauss correlation model is employed to estimate the correlations between two candidates θ_i^1, θ_i^2 for $\hat{P}^1\{\tilde{Z}_{\text{ext}}(\boldsymbol{\theta}_i^1, \boldsymbol{\eta}, T) \le b_\tau\}$ and θ_{ij}^1, θ_{ij}^2 for $\hat{P}^2\{\tilde{Z}_{\text{ext}}(\boldsymbol{\theta}_{i,j}^2, \boldsymbol{\eta}, T) \le b_\tau\}$:

$$R_i = \exp\left(-\omega\left(\theta_i^1 - \theta_i^2\right)^2\right) \tag{27}$$

$$R_{ij} = \prod_{k=1}^{2}\exp\left(-\omega_k\left(\theta_{ij,k}^1 - \theta_{ij,k}^2\right)^2\right) \tag{28}$$

Substituting Eqs. (21), (25) and (26) into Eq. (18), the HDMR model for $P\left\{\tilde{Z}_{\text{ext}}(\boldsymbol{\theta}, \boldsymbol{\eta}, T) \le b_\tau | \boldsymbol{\theta} = \boldsymbol{\theta}_{\text{temp}}\right\}$ is rewritten as:

$$\begin{aligned} &P\left\{\widetilde{Z}_{\text{ext}}(\boldsymbol{\theta}, \boldsymbol{\eta}, T) \le b_\tau \middle| \boldsymbol{\theta} = \boldsymbol{\theta}_{\text{temp}}\right\} \\ &= \sum_{1\le i\le j\le d}\left(\beta_{2,ij} + \mathbf{r}_{ij}^{\mathrm{T}}\left(\boldsymbol{\theta}_{ij}^2\right)\mathbf{R}_{ij}^{-1}\left(\mathbf{Y}_{\mathrm{D},ij}^2 - \mathbf{1}^{\mathrm{T}}\beta_{2,ij}\right)\right) \\ &\quad - (d-1)\sum_{i=1}^{d}\left(\beta_{1,i} + \mathbf{r}_i^{\mathrm{T}}\left(\boldsymbol{\theta}_i^1\right)\mathbf{R}_i^{-1}\left(\mathbf{Y}_{\mathrm{D},i}^1 - \mathbf{1}^{\mathrm{T}}\beta_{1,i}\right)\right) \\ &\quad + \frac{(d-1)(d-2)}{2}P^0\left\{\widetilde{Z}_{\text{ext}}\left(\boldsymbol{\theta}^{\text{med}}, \boldsymbol{\eta}, T\right) \le b_\tau\right\} \end{aligned} \tag{29}$$

With above derivations, the computational consuming of estimation $P\left\{\tilde{Z}_{\text{ext}}(\boldsymbol{\theta}, \boldsymbol{\eta}, T) \le b_\tau | \boldsymbol{\theta} = \boldsymbol{\theta}_{\text{temp}}\right\}$ is substantially relived by combining HDMR and Kriging technique. However, it should be noted that the computational costs of determination of support point set $\mathbf{Y}_{\mathrm{D}}^1$, $\mathbf{Y}_{\mathrm{D}}^2$ and zeroth-order term $P^0\{\tilde{Z}_{\text{ext}}(\boldsymbol{\theta}^{\text{med}}, \boldsymbol{\eta}, T) \le b_\tau\}$ are the still not affordable as discussed in Section 3. Alternatively, the TMSA [43] with finite sampling is employed to overcome the computational barrier of approximation the support point set $\mathbf{Y}_{\mathrm{D}}^1$, $\mathbf{Y}_{\mathrm{D}}^2$ and zeroth-order term $P^0\{\tilde{Z}_{\text{ext}}(\boldsymbol{\theta}^{\text{med}}, \boldsymbol{\eta}, T) \le b_\tau\}$.

4.2. Approximation of the small first passage probability with TMSA

With the advantage of saddle point approximation, TMSA can provide a high accuracy prediction of heavy trail distribution. The main difference of TMSA and other classical saddle point approximation is the weak assumption of the existence of cumulant generating function (CGF) of input variable. Moreover, the lower computational needs of TMSA that only using the first three statistical moment is of importance. In TMSA, the estimation of EVD of $\tilde{Z}_{\text{ext}}^{\text{s}}\left(\boldsymbol{\theta}_{\text{temp}}, \boldsymbol{\eta}, T\right)$ with deterministic structure parameter $\boldsymbol{\theta}_{\text{temp}}$ is expressed as:

$$\begin{aligned} P\left\{\widetilde{Z}_{\text{ext}}\left(\boldsymbol{\theta}_{\text{temp}}, \boldsymbol{\eta}, T\right) \le b_\tau\right\} &= P\left\{\widetilde{Z}_{\text{ext}}^{\text{s}}\left(\boldsymbol{\theta}_{\text{temp}}, \boldsymbol{\eta}, T\right) \le \widetilde{z}_{\text{ext}}\left(b_\tau\right)\right\} \\ &= \begin{cases} \Phi\left\{r_e + \frac{1}{r_e}\ln\left(\frac{q_e}{r_e}\right)\right\} & b_\tau \ne \mu_{\tilde{Z}_{\text{ext}}(\boldsymbol{\theta}_{\text{temp}}, \boldsymbol{\eta}, T)} \\ 0.5 + \alpha^3_{\tilde{Z}_{\text{ext}}^{\text{s}}(\boldsymbol{\theta}_{\text{temp}}, \boldsymbol{\eta}, T)}/6\sqrt{2\pi} & b_\tau = \mu_{\tilde{Z}_{\text{ext}}(\boldsymbol{\theta}_{\text{temp}}, \boldsymbol{\eta}, T)} \end{cases} \end{aligned} \tag{30}$$

$$r_e = \mathrm{sign}\left\{\hat{\xi}\left(b_\tau\right)\right\}\left\{2\left[\hat{\xi}\left(b_\tau\right)\widetilde{z}_{\text{ext}}\left(b_\tau\right) - K_{\tilde{Z}_{\text{ext}}^{\text{s}}(\boldsymbol{\theta}_{\text{temp}}, \boldsymbol{\eta}, T)}\left\{\hat{\xi}\left(b_\tau\right)\right\}\right]\right\}^{1/2} \tag{31}$$

$$q_e = \hat{\xi}\left(b_0\right)\left[K''_{\tilde{Z}_{\text{ext}}^{\text{s}}(\boldsymbol{\theta}_{\text{temp}}, T)}\left\{\hat{\xi}\left(b_0\right)\right\}\right]^{1/2} \tag{32}$$

where, $\tilde{Z}_{\text{ext}}^{\text{s}}\left(\boldsymbol{\theta}_{\text{temp}}, \boldsymbol{\eta}, T\right) = \left(\tilde{Z}_{\text{ext}}\left(\boldsymbol{\theta}_{\text{temp}}, \boldsymbol{\eta}, T\right) - \mu_{\tilde{Z}_{\text{ext}}(\boldsymbol{\theta}_{\text{temp}}, \boldsymbol{\eta}, T)}\right)/\sigma_{\tilde{Z}_{\text{ext}}(\boldsymbol{\theta}_{\text{temp}}, \boldsymbol{\eta}, T)}$ and $\tilde{Z}_{\text{ext}}\left(b_\tau\right) = \left(b_\tau - \mu_{\tilde{Z}_{\text{ext}}(\boldsymbol{\theta}_{\text{temp}}, \boldsymbol{\eta}, T)}\right)/\sigma_{\tilde{Z}_{\text{ext}}(\boldsymbol{\theta}_{\text{temp}}, \boldsymbol{\eta}, T)}$ denote the standardized form of $\tilde{Z}_{\text{ext}}\left(\boldsymbol{\theta}_{\text{temp}}, \boldsymbol{\eta}, T\right)$ and b_τ; $\mu_{\tilde{Z}_{\text{ext}}(\boldsymbol{\theta}_{\text{temp}}, \boldsymbol{\eta}, T)}$ and $\sigma_{\tilde{Z}_{\text{ext}}(\boldsymbol{\theta}_{\text{temp}}, \boldsymbol{\eta}, T)}$ denote the mean and standard variation of variable $\tilde{Z}_{\text{ext}}\left(\boldsymbol{\theta}_{\text{temp}}, \boldsymbol{\eta}, T\right)$. The saddle point $\hat{\xi}\left(b_\tau\right)$ is expressed as:

$$\hat{\xi}\left(b_\tau\right) = 2\widetilde{Z}_{\text{ext}}\left(b_\tau, T\right)/\left(2 + \gamma_{\tilde{Z}_{\text{ext}}^{\text{s}}(\boldsymbol{\theta}_{\text{temp}}, \boldsymbol{\eta}, T)}\widetilde{Z}_{\text{ext}}\left(b_\tau, T\right)\right) \tag{33}$$

in which, $\gamma_{\tilde{Z}_{\text{ext}}^{\text{s}}(\boldsymbol{\theta}_k, \boldsymbol{\eta}, T)} = E\left(\tilde{Z}_{\text{ext}}\left(\boldsymbol{\theta}_{\text{temp}}, \boldsymbol{\eta}, T\right) - \mu_{\tilde{Z}_{\text{ext}}(\boldsymbol{\theta}_{\text{temp}}, \boldsymbol{\eta}, T)}\right)^3/\sigma^3_{\tilde{Z}_{\text{ext}}(\boldsymbol{\theta}_{\text{temp}}, \boldsymbol{\eta}, T)}$ is represented the skewness of standard variable $\tilde{Z}_{\text{ext}}^{\text{s}}\left(\boldsymbol{\theta}_{\text{temp}}, \boldsymbol{\eta}, T\right)$. Given the value of $\hat{\xi}\left(b_\tau\right)$ the CGF $K_{\tilde{Z}_{\text{ext}}^{\text{s}}(\boldsymbol{\theta}_{\text{temp}}, \boldsymbol{\eta}, T)} \times \left\{\hat{\xi}\left(b_\tau\right)\right\}$ and $K''_{\tilde{Z}_{\text{ext}}^{\text{s}}(\boldsymbol{\theta}_{\text{temp}}, \boldsymbol{\eta}, T)}\left\{\hat{\xi}\left(b_\tau\right)\right\}$ the second derivation of CGF is written as:

$$K_{\tilde{Z}_{\text{ext}}^{\text{s}}(\boldsymbol{\theta}_{\text{temp}}, \boldsymbol{\eta}, T)}\left\{\hat{\xi}\left(b_\tau\right)\right\} = \begin{cases} -2\hat{\xi}\left(b_\tau\right)/\gamma_{\tilde{Z}_{\text{ext}}^{\text{s}}(\boldsymbol{\theta}_{\text{temp}}, \boldsymbol{\eta}, T)} - 2\ln\left\{\left(1 - \gamma_{\tilde{Z}_{\text{ext}}^{\text{s}}(\boldsymbol{\theta}_{\text{temp}}, \boldsymbol{\eta}, T)}\hat{\xi}\left(b_\tau\right)/2\right)^2\right\} & \gamma_{\tilde{Z}_{\text{ext}}^{\text{s}}(\boldsymbol{\theta}_{\text{temp}}, \boldsymbol{\eta}, T)} \ne 0 \\ 0.5\hat{\xi}^2\left(b_\tau\right) & \gamma_{\tilde{Z}_{\text{ext}}^{\text{s}}(\boldsymbol{\theta}_{\text{temp}}, \boldsymbol{\eta}, T)} = 0 \end{cases} \tag{34}$$

$$K''_{\tilde{Z}_{\text{ext}}^{\text{s}}(\boldsymbol{\theta}_{\text{temp}}, \boldsymbol{\eta}, T)}\left\{\hat{\xi}\left(b_\tau\right)\right\} = 1/\left\{1 - 0.5\gamma_{\tilde{Z}_{\text{ext}}^{\text{s}}(\boldsymbol{\theta}_{\text{temp}}, \boldsymbol{\eta}, T)}\hat{\xi}\left(b_\tau\right)\right\}^2 \tag{35}$$

As shown in above formulations, the TMSA only needs the first three statistical moment to predict the uncertain distribution of variables. Consider the hundreds even thousands components in aleatory vector $\boldsymbol{\eta}$, the first three statistical moments are obtained by several thousands of simulations with good convergence for estimation of $\mathbf{Y}_{\mathrm{D}}^{1}$, $\mathbf{Y}_{\mathrm{D}}^{2}$ and zeroth-order term $P^{0}\{\tilde{Z}_{\mathrm{ext}}(\boldsymbol{\theta}^{\mathrm{med}},\boldsymbol{\eta},T) \le b_{\tau}\}$. As depicted in this section, the combination of Kriging-HDMR and TMSA is employed to construct the meta-model of the estimation of conditional EVD $P\{\tilde{Z}_{\mathrm{ext}}(\boldsymbol{\theta},\boldsymbol{\eta},T) \le b_{\tau}|\boldsymbol{\theta} = \boldsymbol{\theta}_{\mathrm{temp}}\}$. By constructing the meta-model, the estimation of $P\left\{\tilde{Z}_{\mathrm{ext}}\left(\boldsymbol{\theta}_{\mathrm{temp}},\boldsymbol{\eta},T\right) \le b_{\tau}\right\}$ is transformed to the approximation of $P\left\{\tilde{Z}_{\mathrm{ext}}\left(\boldsymbol{\theta}_{\mathrm{temp}}\right) \le b_{\tau}\right\}$. In other words, the process of estimation of $P\left\{\tilde{Z}_{\mathrm{ext}}\left(\boldsymbol{\theta},\boldsymbol{\eta},T\right) \le b_{\tau}\right\}$ is converted to the uncertainty quantification of $\boldsymbol{\theta}$ corresponding to the meta-model. The uncertainty propagation of $\boldsymbol{\theta}$ is discussed in Section 5.

5. Estimation bounds of EVD

As mentioned in above sections, the uncertainties rooted in structural parameters are depicted with interval theory. Therefore, the estimation of LB and UB of $P\left\{\tilde{Z}_{\mathrm{ext}}\left(\boldsymbol{\theta}^{\mathrm{I}},\boldsymbol{\eta},T\right) \le b_{\tau}\right\}$ is expressed as the process of searching the maximum and minimum value of system response in the d-dimensional hypercube space $\mathbf{V}\left(\boldsymbol{\theta}\right) = \left[\underline{\theta}_1,\overline{\theta}_1\right] \times \left[\underline{\theta}_2,\overline{\theta}_2\right] \times,\ldots,\times \left[\underline{\theta}_d,\overline{\theta}_d\right]$. From the traditional view, the solution of two bounds constrained problem $P\left\{\tilde{Z}_{\mathrm{ext}}\left(\boldsymbol{\theta}^{\mathrm{I}},\boldsymbol{\eta},T\right) \le b_{\tau}\right\}$ is obtained by MC simulation. However, MC simulation with the high degree of accuracy may become computationally very extensive. To alleviate the computational burden, the differential evolution (DE) interval optimization technique is used to estimate the LB and UB of $P\left\{\tilde{Z}_{\mathrm{ext}}\left(\boldsymbol{\theta}^{\mathrm{I}},\boldsymbol{\eta},T\right) \le b_{\tau}\right\}$. DE is a stochastic population-based search method developed by [44] and has been effectively used to uncertainty quantification [47,48] and structural optimization [49] by authors. With the mutation, crossover and selection operations, DE may give a robust search result with fast convergence. The concrete description of DE is documented in [44,50].

5.1. Uncertainty propagation using DE

The estimation of LB and UB of $P\left\{\tilde{Z}_{\mathrm{ext}}\left(\boldsymbol{\theta},\boldsymbol{\eta},T\right) \le b_{\tau}\right\}$ is expressed as the process of searching the minimum and maximum value of objective function subject to sample space $\underline{\boldsymbol{\theta}} \le \boldsymbol{\theta}_{\mathrm{temp}} \le \overline{\boldsymbol{\theta}}$. From Eq. (29), we can find that the constant terms of meta-model make no contributions to the variation of $P\left\{\tilde{Z}_{\mathrm{ext}}\left(\boldsymbol{\theta},\boldsymbol{\eta},T\right) \le b_{\tau}\right\}$. Then, the objective functions of optimization process for $\underline{P}\left\{\tilde{Z}_{\mathrm{ext}}\left(\boldsymbol{\theta}^{\mathrm{I}},\boldsymbol{\eta},T\right) \le b_{\tau}\right\}$ and $\overline{P}\left\{\tilde{Z}_{\mathrm{ext}}\left(\boldsymbol{\theta}^{\mathrm{I}},\boldsymbol{\eta},T\right) \le b_{\tau}\right\}$ are rewritten as Eqs. (36)–(37) in Box I: As shown in Eqs. (36)–(37), the conventional optimization algorithms are computationally efficient in general, but maybe trapped in local extreme value of objective functions. Herein we use DE to search the global optimal value of objective function. Similar to other evolution algorithms, DE starts with the stochastic sampling in variable space $\mathbf{V}\left(\boldsymbol{\theta}\right) = \left[\underline{\theta}_1,\overline{\theta}_1\right] \times \left[\underline{\theta}_2,\overline{\theta}_2\right] \times,\ldots,\times \left[\underline{\theta}_d,\overline{\theta}_d\right]$. The mutation and crossover operations guarantee its robustness and diversity throughout the variable space. Compare to conventional optimization algorithms, the main advantage of DE is its selection strategy. The greedy criterion as shown in Eq. (38) is employed to search the best individual between the competitors:

$$\boldsymbol{\theta}_{G+1} = \begin{cases} \boldsymbol{\theta}_G^{\mathrm{c}} & if\ \left(\mathrm{obj}\left(\boldsymbol{\theta}_G^{\mathrm{c}}\right) < \mathrm{obj}\left(\boldsymbol{\theta}_G\right)\right) \\ \boldsymbol{\theta}_G & \text{otherwise} \end{cases} \tag{38}$$

where $\boldsymbol{\theta}_{G+1}$ denotes the updated individual; $\boldsymbol{\theta}_G$ and $\boldsymbol{\theta}_G^{\mathrm{c}}$ denote the old individual and competitor, respectively. The competitions not only exist in offspring generations but between offspring and its parents. Thus, the better individual will pass to the next generation until the optimal results are obtained. According to Eqs. (36)–(37), the LB and UB of $P\left\{\tilde{Z}_{\mathrm{ext}}\left(\boldsymbol{\theta}^{\mathrm{I}},\boldsymbol{\eta},T\right) \le b_{\tau}\right\}$ can be expressed as:

$$\left[\underline{P}\left\{\widetilde{Z}_{\mathrm{ext}}\left(\boldsymbol{\theta}^{\mathrm{I}},\boldsymbol{\eta},T\right) \le b_{\tau}\right\}, \overline{P}\left\{\widetilde{Z}_{\mathrm{ext}}\left(\boldsymbol{\theta}^{\mathrm{I}},\boldsymbol{\eta},T\right) \le b_{\tau}\right\}\right]$$
$$= \left[P\left\{\widetilde{Z}_{\mathrm{ext}}\left(\boldsymbol{\theta}_{\mathrm{temp},1},\boldsymbol{\eta},T\right) \le b_{\tau}\right\}, P\left\{\widetilde{Z}_{\mathrm{ext}}\left(\boldsymbol{\theta}_{\mathrm{temp},2},\boldsymbol{\eta},T\right) \le b_{\tau}\right\}\right] \tag{39}$$

Substituting the Eq. (39) into the Eq. (7), the LB and UB of first passage probability $P_f\left(\boldsymbol{\theta}^{\mathrm{I}},\boldsymbol{\eta},b_{\tau},T\right)$ is obtained.

5.2. Framework of dynamic reliability with epistemic uncertainty

Based on the above discussion, the proposed Kriging-HDMR together with TMSA is implemented as following steps:

Step 1. Determine the interval range of uncertain structural parameters and support point for zeroth-order term of HDMR;

Step 2. Identify the number of random uncertainties in stochastic excitation η.

Step 3. Generate the sample input of first and second order terms of HDMR.

Step 4. Use randomness variable that generated by the identified in Step 2 to determine N time series with the quasi-Monte-Carlo simulations. Repeat the time history analysis for the structure with designate parameters under these excitation series.

Step 5. Estimate the conditional EVD of $\tilde{Z}_{\mathrm{ext}}\left(\boldsymbol{\theta}_{\mathrm{temp}},\boldsymbol{\eta},T\right)$ and construct the Kriging models for first and second order HDMR approximation, respectively.

Step 6. Perform DE interval optimization to determine the LB and UB of $P\left\{\tilde{Z}_{\mathrm{ext}}\left(\boldsymbol{\theta},\boldsymbol{\eta},T\right) \le b_{\tau}\right\}$.

The above outlined analytical process of dynamic reliability of structural system is illustrated in Fig. 1.

6. Case study

The nine-story shear structure [51], as shown in Fig. 2, is considered here to investigate the efficiency and effectiveness of proposed in this work. The nominal value of stiffness and lumped mass of each story as shown in Table 1. The Rayleigh damping $\mathbf{C}\left(\boldsymbol{\theta}\right) = c_0\mathbf{M}\left(\boldsymbol{\theta}\right) + c_1\mathbf{K}\left(\boldsymbol{\theta}\right)$ is used here to denote energy dissipation. The corresponding parameters $c_0 = 0.3843\mathrm{s}^{-1}$ and $c_1 = 0.0052\mathrm{s}$ are given by assuming the mode damping ratio $\xi = 0.05$ for the first and second modes. The nonlinear relationship of restoring force and inter-story drift is characterized by the classical Bouc–Wen model [52]:

$$\mathbf{M}(\boldsymbol{\theta})\ddot{\mathbf{X}}\left(\boldsymbol{\theta},\boldsymbol{\eta},t\right) + \mathbf{C}(\boldsymbol{\theta})\dot{\mathbf{X}}\left(\boldsymbol{\theta},\boldsymbol{\eta},t\right) + \mathbf{K}(\boldsymbol{\theta})\left[\alpha\mathbf{X}\left(\boldsymbol{\theta},\boldsymbol{\eta},t\right) + (1-\alpha)\,\mathbf{Z}\left(\boldsymbol{\theta},\boldsymbol{\eta},t\right)\right]$$
$$= \mathbf{M}(\boldsymbol{\theta})\ddot{x}_g\left(\boldsymbol{\eta},t\right) \tag{40}$$

$$\Delta\dot{\mathbf{Z}}\left(\boldsymbol{\theta},\boldsymbol{\eta},t\right) = -\gamma\left|\Delta\dot{\mathbf{X}}\left(\boldsymbol{\theta},\boldsymbol{\eta},t\right)\right|\Delta\mathbf{Z}\left(\boldsymbol{\theta},\boldsymbol{\eta},t\right)\left|\Delta\mathbf{Z}\left(\boldsymbol{\theta},\boldsymbol{\eta},t\right)\right|^{n_0-1}$$
$$-\ \beta\Delta\dot{\mathbf{X}}\left(\boldsymbol{\theta},\boldsymbol{\eta},t\right)\left|\Delta\mathbf{Z}\left(\boldsymbol{\theta},\boldsymbol{\eta},t\right)\right|^{n_0} + A\Delta\dot{\mathbf{X}}\left(\boldsymbol{\theta},\boldsymbol{\eta},t\right) \tag{41}$$

where, $\mathbf{K}\left(\boldsymbol{\theta}\right)$ is the initial stiffness matrix of structural system; $\Delta\dot{\mathbf{X}}\left(\boldsymbol{\theta},\boldsymbol{\eta},T\right)$ and $\Delta\mathbf{X}\left(\boldsymbol{\theta},\boldsymbol{\eta},T\right)$ are the inter-story velocity and drift vectors, respectively; $\mathbf{Z}\left(\boldsymbol{\theta},\boldsymbol{\eta},T\right)$ is the hysteretic displacement vector; $\Delta\dot{\mathbf{Z}}\left(\boldsymbol{\theta},\boldsymbol{\eta},T\right)$ and $\Delta\mathbf{Z}\left(\boldsymbol{\theta},\boldsymbol{\eta},T\right)$ are the inter-story velocity and drift vectors of hysteretic system, respectively. The Bouc–Wen parameters: $A = n_0 = 1.0$; the nominal value of $\gamma = 40$, $\beta = 20$. The seismic excitation $\ddot{x}_g\left(\boldsymbol{\eta},t\right)$ is modeled by a non-stationary filtered white noise process and corresponding power spectral density is denoted by the Kanai–Tajimi model:

$$S_{ff}\left(\omega\right) = S_0\frac{4\zeta_g^2\omega_g^2\omega^2 + \omega_g^4}{\left(\omega_g^2 - \omega^2\right)^2 + 4\zeta_g^2\omega_g^2\omega^2} \tag{42}$$

in which, the constant power spectral density intensity of the bed rock $S_0 = 0.0156\ \mathrm{m}^2/\mathrm{s}^3$, the factor $\xi_g = 0.6$ is used here to denote the efficient damping ratio of the ground, and ground frequency $\omega_{\mathrm{g}} = 4\pi$ rad/s.

$$
\begin{aligned}
&find && \boldsymbol{\theta}_{\text{temp},1} \\
&\text{minmize} && \sum_{1\le i\le j\le d} \mathbf{r}_{ij}^{\mathrm{T}}(\boldsymbol{\theta})\,\mathbf{R}_{ij}^{-1}\left(\mathbf{Y}_{\mathrm{D},ij}^{2}-\mathbf{1}^{\mathrm{T}}\beta_{2,ij}\right)-(d-1)\sum_{i=1}^{d}\mathbf{r}_{i}^{\mathrm{T}}(\boldsymbol{\theta})\,\mathbf{R}_{i}^{-1}\left(\mathbf{Y}_{\mathrm{D},i}^{1}-\mathbf{1}^{\mathrm{T}}\beta_{1,i}\right) \qquad (36)\\
&s.t. && \boldsymbol{\theta}_{\text{temp},1}\in\left[\underline{\boldsymbol{\theta}},\overline{\boldsymbol{\theta}}\right] \\
&find && \boldsymbol{\theta}_{\text{temp},2} \\
&\text{minmize} && -\sum_{1\le i\le j\le d} \mathbf{r}_{ij}^{\mathrm{T}}(\boldsymbol{\theta})\,\mathbf{R}_{ij}^{-1}\left(\mathbf{Y}_{\mathrm{D},ij}^{2}-\mathbf{1}^{\mathrm{T}}\beta_{2,ij}\right)+(d-1)\sum_{i=1}^{d}\mathbf{r}_{i}^{\mathrm{T}}(\boldsymbol{\theta})\,\mathbf{R}_{i}^{-1}\left(\mathbf{Y}_{\mathrm{D},i}^{1}-\mathbf{1}^{\mathrm{T}}\beta_{1,i}\right) \qquad (37)\\
&s.t. && \boldsymbol{\theta}_{\text{temp},2}\in\left[\underline{\boldsymbol{\theta}},\overline{\boldsymbol{\theta}}\right]
\end{aligned}
$$

Box I.

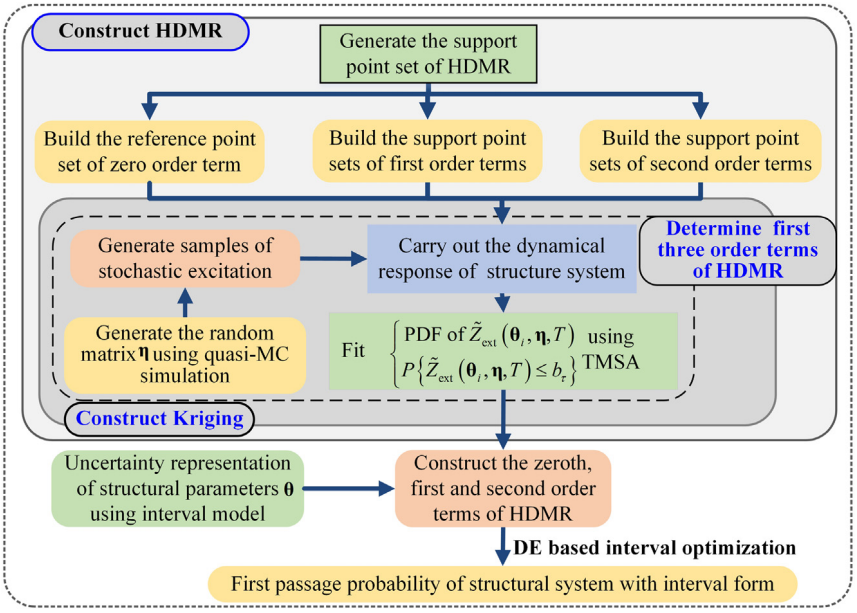

Fig. 1. Flowchart of dynamic reliability analysis of structure system with epistemic uncertainties.

Spectral representation method [6,7] is used here to express the time domain nonstationary process as shown in following:

$$\ddot{x}_g(t)=g(t)\left[\sqrt{2}\sum_{i=1}^{N}A_i\cos\left(\omega_i t+\varphi_i\right)\right] \qquad (43)$$

where, the amplitude $A_i=\sqrt{2S_{ff}(\omega_i)\,\Delta\omega}$, $\omega_i=i\Delta\omega$ and $N=\omega_{\text{upper}}/\Delta\omega$; the upper cut frequency $\omega_{\text{upper}}=100$ rad/s, the equal frequency interval $\Delta\omega=0.2$ rad/s. The uniform modulate function $g(t)$ is used here to denote the intensity variation based on time:

$$g(t)=\begin{cases}(t/t_a)^2 & 0\le t\le t_a\\ 1 & t_a<t\le t_b\\ \exp\left[-\beta\left(t-t_b\right)\right] & t_b<t\le T\\ 0 & t>T\end{cases}, \qquad (44)$$

where $t_a=1$ s and $t_b=7$ s are the start and end time of stationary part of stochastic process; $\beta=0.35$ is the attenuation ratios of the stationary section. The 4th order Runge–Kutta method is used here to compute the dynamic response of nine-story shear structure under the excited with the generated artificial acceleration. The time step is designated as $\Delta t=0.02$ s, and the time span is determined as 15 s.

Table 1
Mean value of lumped mass and inter-story stiffness.

Story No.	1	2	3	4	5	6	7	8	9
Mass($\times10^5$ kg)	3.442	3.278	3.056	2.756	2.739	2.739	2.739	2.739	2.692
Stiffness ($\times10^5$ N/m)	3.7	3.4	3.0	2.8	2.6	2.4	2.0	1.6	1.0

6.1. Deterministic value of structural parameters

In the first case, the structural properties, including the story mass, stiffness, and parameters of Bouc–Wen model are assumed as deterministic. The uncertainty involved in dynamic analysis is the randomness of external excitation. The inter-story drift $\Delta\mathbf{X}(\boldsymbol{\theta},\boldsymbol{\eta},T)$ is considered quantities of interest. Then, the probability density function (PDF) of $\widetilde{\Delta\mathbf{X}}_{\text{ext}}(\boldsymbol{\theta},\boldsymbol{\eta},T)$ and corresponding first passage probability of $\Delta\mathbf{X}(\boldsymbol{\theta},\boldsymbol{\eta},T)$ is represented as $1-P\left\{\widetilde{\Delta\mathbf{X}}_{\text{ext}}(\boldsymbol{\theta},\boldsymbol{\eta},T)\le b_\tau\right\}$. The correlation-reduction Latin hypercube sampling (CLHS) [53] method is used here to generate the sampling. A 2500 numbers of CLHS is generated to obtain the first three moment of dynamic system response. To investigate the accuracy and efficiency of the obtained dynamic reliability by using TMSA, a 10^6 MC simulations is employed to act the baseline as shown in Fig. 3. In comparison with the efficiency and accuracy of CLHS-TMSA results, the TMSA estimation of the PDF of EVD and the first passage probability with 10^6 MC simulations also

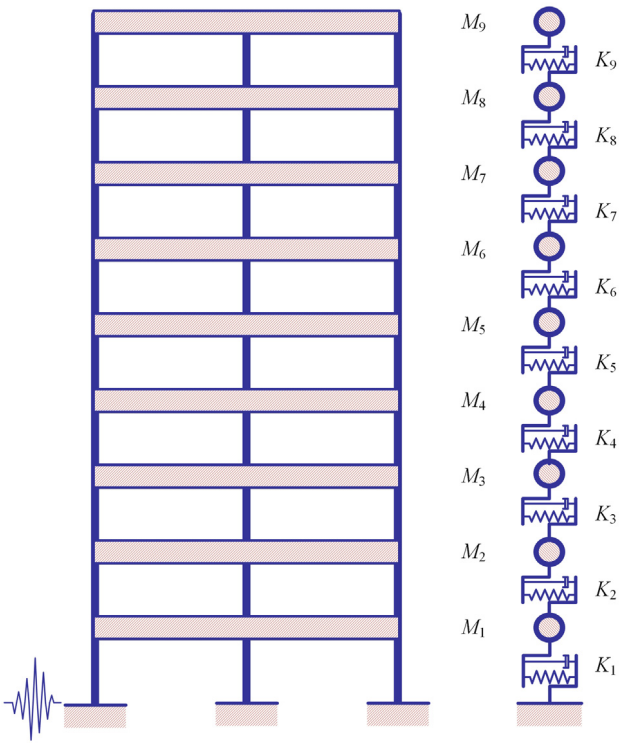

Fig. 2. The story-shear structure.

plotted in Fig. 3(a) and (b), respectively. The $P_f\left(b_\tau, 15\text{s}\right)$ in Fig. 3(b) is the short note of $P_f\left(\boldsymbol{\theta}, \boldsymbol{\eta}, b_\tau, 15\text{s}\right)$.

From Fig. 3(a), the fairly close agreement of CLHS-TMSA result with 2500 samples and MC simulation result with 10^6 samples demonstrate the proposed method captures the characters of the EVD of $\widetilde{\Delta\mathbf{X}}_{\text{ext}}\left(\boldsymbol{\theta}, \boldsymbol{\eta}, T\right)$. As shown in Fig. 3(b), the estimated first passage probability of inter-story drift obtained by TMSA with 2500 CLHS simulations is well matched with the results given by 10^6 direct MC simulations at the range of threshold value [0.01 m, 0.06 m]. While, the first passage probability of inter-story obtained by direct Monte-Carlo simulations is effective and accurate for the probability larger than $10^{-4} \sim 10^{-5}$. Moreover, the first passage probability of inter-story drift obtained by TMSA with 2500 CLHS simulations is well agree with the estimated results obtained by TMSA with 10^6 Monte-Carlo simulations for the large threshold value. From above comparison, we can conclude that the proposed methodology for the TMSA provide a meaningful measure for small passage probabilities as low as 10^{-8}, even the numbers of sampling are not sufficiently large.

6.2. Dependent uncertain parameter with interval numbers

In the second scenario, we assume the dependent variable lumper mass matrix $\mathbf{M}(\boldsymbol{\theta})$ and the Bouc–Wen model parameters α, β, γ of each story are interval formed. The interval uncertain degree ν of uncertain vector $\boldsymbol{\theta}^{\text{I}} = \left[\theta_{\boldsymbol{M}}^{\text{I}}, \theta_\alpha^{\text{I}}, \theta_\beta^{\text{I}}, \theta_\gamma^{\text{I}}\right]^{\text{T}}$ is assumed as 0.05, 0.1, 0.15 and 0.2. Then, the element expression of LB and UB of $\boldsymbol{\theta}^{\text{I}}$ is defined as:

$$\left[\underline{\boldsymbol{\theta}}, \overline{\boldsymbol{\theta}}\right] = \left[(1-\nu)\left[\theta_{\mathbf{M}}^{\text{med}}, \theta_\alpha^{\text{med}}, \theta_\beta^{\text{med}}, \theta_\gamma^{\text{med}}\right]^{\text{T}}, (1+\nu)\left[\theta_{\mathbf{M}}^{\text{med}}, \theta_\alpha^{\text{med}}, \theta_\beta^{\text{med}}, \theta_\gamma^{\text{med}}\right]^{\text{T}}\right] \tag{45}$$

where, θ_i^{med} is the median value of θ_i. From the above Section 6.1, it seemed that the computational needs of EVD computation is evidently released by using the CLHS-TMSA for deterministic parameters of structure. While, the computational burden of dynamic reliability involving in epistemic may be extremely increased due to the computational consuming of interval extreme value. To solve this problem, the Kriging assistant HDMR is used here to act the response surface of first passage probability of inter-story drift of structure system $\Delta\mathbf{X}\left(\boldsymbol{\theta}, \boldsymbol{\eta}, T\right)$. It is well known that the accuracy and computational efficiency are tradeoff for each other.

6.2.1. Construction and test of the HDMR

The first order and second order expansion of HDMRs are constructed in uncertain domain $\boldsymbol{\theta}^{\text{I}}$ with four support points in each dimension. Correspondingly, the conditional EVD of each support point is determined by TMSA with 2500 CHLS simulations. The first passage probability $P_f\left(b_\tau, 15s\right)$ with the structural parameter vector $\underline{\boldsymbol{\theta}}$ and $\overline{\boldsymbol{\theta}}$ are used here to study the accuracy and efficiency of first order and second order HDMRs for the uncertain level of structural parameter are 0.05, 0.1, 0.15 and 0.2. The investigation results are shown in Fig. 4. The TMSA approximation with 2500 CHLS simulations is used here to act the reference one.

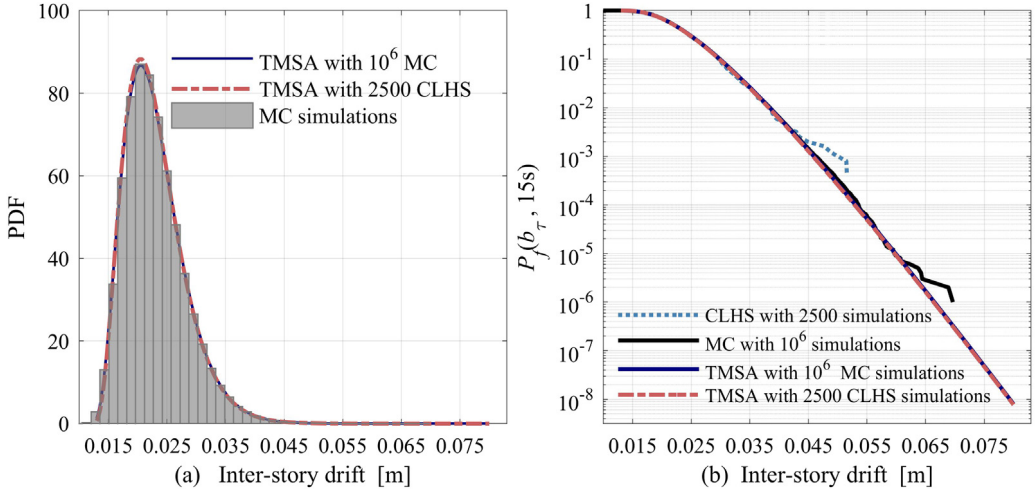

Fig. 3. (a) EVD and (b) first passage probability of inter-story drift with deterministic structure parameters.

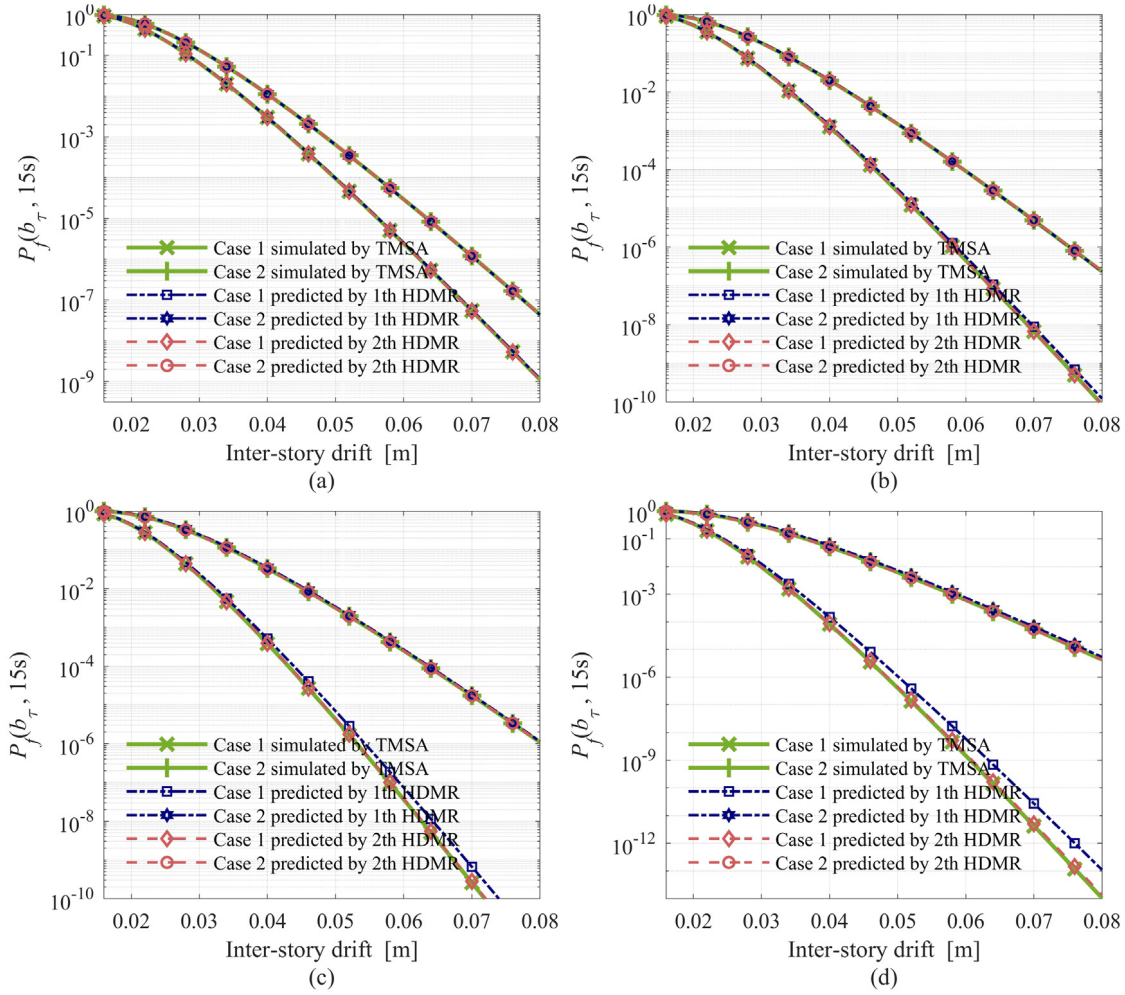

Fig. 4. Comparison the accuracy of first order HDMR and second order HDMR prediction with (a) uncertain level $\nu = 0.05$; (b) uncertain level $\nu = 0.1$; (c) uncertain level $\nu = 0.15$ (d) uncertain level $\nu = 0.2$ of structural parameters.

As shown in Fig. 4(a), both first order and second order HDMR gives a precise approximation results for the prediction $P_f\left(b_\tau, 15\text{ s}\right)$ corresponding to $\underline{\boldsymbol{\theta}}$ and $\overline{\boldsymbol{\theta}}$ for the uncertain level $\nu = 0.05$. However, the scenario of the uncertain level $\nu = 0.1$ as shown in Fig. 4(b) demonstrated that the prediction accuracy of first order HDMR for the LB of $P_f\left(b_\tau, 15\text{ s}\right)$ is decreased with the increase of threshold value b_τ. In other words, the first order HDMR gives a non-conservative prediction results for the LB of first passage probability when the uncertain level $\nu = 0.1$. The Fig. 4(c) and (d) show that the prediction of second order HDMR is well matched with the simulation result of TMSA with 2500 CLHS sampling. Especially, the distinction between the prediction value of first order HDMR and the simulation of TMSA is evidently enlarged with the increment of threshold value of b_τ. This means that the prediction first passage probability with first order HDMR is not applicable for the small value of $\underline{P}_f\left(b_\tau, 15\text{ s}\right)$ corresponding to $\nu = 0.15$ and $\nu = 0.2$. Thus, the prediction frame using second order HDMR is employed in subsequent prediction of bounds value of first passage probability P_f with large uncertain level.

6.2.2. Estimation of the LB and UB of first passage probability

As discussed above, the second order HDMR may give a more accurate estimation result for the first passage probability of inter-story drift $\Delta\mathbf{X}\left(\boldsymbol{\theta}, \boldsymbol{\eta}, T\right)$. Therefore, the second order HDMR based probability response surface is employed to approximate the LB and UB of $P_f\left(b_\tau, 15\text{ s}\right)$. After the construction of meta-model, the DE interval optimization algorithm is used to estimate the LB and UB of $P_f\left(b_\tau, 15\text{ s}\right)$. The initial population and maximum number of iterations are designated as 30 and 50, respectively. The MC simulations with 10^4 and 10^5 sampling are also implemented here to investigate the efficiency of DE-HDMR method as shown in Fig. 5. The LB and UB of $P_f\left(b_\tau, 15\text{ s}\right)$ in Fig. 5(a), (b), (c) and (d) are corresponding to the uncertain level $\nu = 0.05$, $\nu = 0.1$, $\nu = 0.15$ and $\nu = 0.2$.

As shown in Fig. 5(a) and (b), the LB and UB results predicted by DE are well agree with MC simulation with 10^4 and 10^5 samples at the uncertain level $\nu = 0.05$ and $\nu = 0.1$. Compare Fig. 5(c) and (d) with above two subfigures, the estimation with DE gives a more wider approximation range of the LB and UB of $P_f\left(b_\tau, 15\text{ s}\right)$. This demonstrates that the predicted result of post process DE gives a more robust estimation of the $\underline{P}_f\left(b_\tau, 15\text{ s}\right)$ and $\overline{P}_f\left(b_\tau, 15\text{ s}\right)$. To investigate above discussion by numerical form, Tables 2–3 are used to collect the LB and UB values of $P_f\left(b_\tau, 15\text{ s}\right)$ by fixing the threshold value $b_\tau = 0.06$ m and 0.08 m at the uncertain level $\nu = 0.05, 0.1, 0.15$ and 0.2.

From a more detailed comparison of these three different post processes as allocated in Table 2, the difference between the MC simulation with 10^4 sampling and DE post process larger than 11%, 15%, 50% and 111% for the $\underline{P}_f\left(0.06\text{ m}, 15\text{ s}\right)$ with uncertain level $\nu = 0.05, 0.1, 0.15$ and 0.2; the difference is larger than 7.7%, 13.2%, 12.7% and 24% for $\overline{P}_f\left(0.06\text{ m}, 15\text{ s}\right)$ with uncertain level $\nu = 0.05, 0.1, 0.15$ and 0.2, respectively. As reflected in Table 3, the difference of MC simulation with 10^4 samples and DE is larger than 17.4%, 26%, 92% even 171.2% for the $\underline{P}_f\left(0.08\text{ m}, 15\text{ s}\right)$ with the uncertain level$\nu = 0.05, 0.1, 0.15$ and 0.2, respectively. From above comparison, it can be

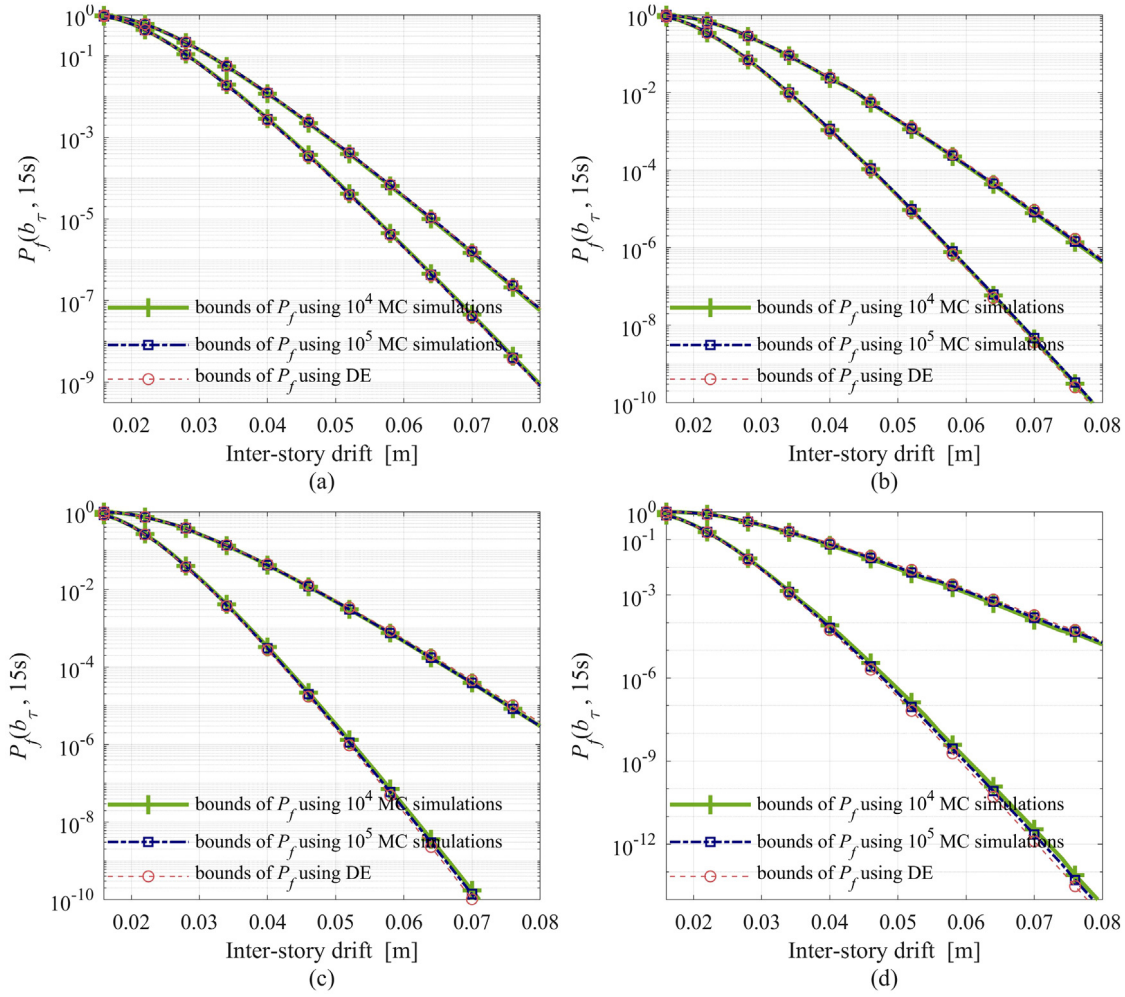

Fig. 5. Comparison the prediction of $\underline{P}_f(b_\tau, 15\text{ s})$ and $\overline{P}_f(b_\tau, 15\text{ s})$ using MC simulation with 10^4 and 10^5 samples and DE simulation with (a) uncertain level $\nu = 0.05$; (b) uncertain level $\nu = 0.1$; (c) uncertain level $\nu = 0.15$ and (d) uncertain level $\nu = 0.2$ of structural parameters.

Table 2
Comparison the LB and UB of $P_f(b_\tau, 15\text{ s})$ corresponding to $b_\tau = 0.06$ m under uncertain level $\nu = 0.05, 0.1$ and 0.2 with different post process of prediction.

Uncertain level ν		10^4 MC	10^5 MC	DE
0.05	LB	2.113×10^{-6}	2.001×10^{-6}	$\mathbf{1.905\times10^{-6}}$
	UB	3.471×10^{-5}	3.667×10^{-5}	$\mathbf{3.760\times10^{-5}}$
0.1	LB	3.265×10^{-7}	3.425×10^{-7}	$\mathbf{2.833\times10^{-7}}$
	UB	1.288×10^{-4}	1.351×10^{-4}	$\mathbf{1.484\times10^{-4}}$
0.15	LB	2.644×10^{-8}	2.213×10^{-8}	$\mathbf{1.760\times10^{-8}}$
	UB	4.572×10^{-4}	4.604×10^{-4}	$\mathbf{5.238\times10^{-4}}$
0.2	LB	1.215×10^{-9}	8.718×10^{-10}	$\mathbf{5.755\times10^{-10}}$
	UB	0.00119	0.00137	**0.00156**

Table 3
Comparison the LB and UB of $P_f(b_\tau, 15\text{ s})$ corresponding to $b_\tau = 0.08$ m under uncertain level $\nu = 0.05, 0.1$ and 0.2 with different post process of prediction.

Uncertain level ν		10^4 MC	10^5 MC	DE
0.05	LB	8.865×10^{-10}	8.130×10^{-10}	$\mathbf{7.552\times10^{-10}}$
	UB	5.743×10^{-8}	6.265×10^{-8}	$\mathbf{6.509\times10^{-8}}$
0.1	LB	5.209×10^{-11}	5.583×10^{-11}	$\mathbf{4.123\times10^{-11}}$
	UB	4.198×10^{-7}	4.518×10^{-7}	$\mathbf{5.237\times10^{-7}}$
0.15	LB	1.001×10^{-12}	7.608×10^{-13}	$\mathbf{5.215\times10^{-13}}$
	UB	2.962×10^{-6}	2.952×10^{-6}	$\mathbf{3.670\times10^{-6}}$
0.2	LB	6.664×10^{-15}	4.275×10^{-15}	$\mathbf{2.457\times10^{-15}}$
	UB	1.632×10^{-5}	1.891×10^{-5}	$\mathbf{2.220\times10^{-5}}$

found that the difference of $\overline{P}_f(b_\tau, 15\text{ s})$ is smaller than and $\underline{P}_f(b_\tau, 15\text{ s})$. The main reason for this scenario is the variation of small value of probability is more sensitivity than large value. In other words, the DE interval optimization technique gives a more robust bounds of first passage probability compare to MC simulation. After the discussion of the accuracy and efficiency of proposed method, the sensitivity analysis of first passage probability of inter-story drift corresponding to the interval uncertainties in structural parameters is investigated.

6.2.3. Sensitivity of each uncertain parameter

The first passage probability of dynamic system is characterized by the small value, which always be depicted in semi-logarithmic coordinates. Then, the sensitivity index defined in this work is based on the logarithmic representation of first passage probability. According to the definition of interval theory, the radius of interval based first passage probability $P_f^{\text{rad}}(\boldsymbol{\theta}^{\text{I}}, \boldsymbol{\eta}, b_\tau, T)$ is expressed as:

$$P_f^{\text{rad}}(\boldsymbol{\theta}^{\text{I}}, \boldsymbol{\eta}, b_\tau, T) = \log 10\left\{\overline{P}_f(\boldsymbol{\theta}^{\text{I}}, \boldsymbol{\eta}, b_\tau, T)/\underline{P}(\boldsymbol{\theta}^{\text{I}}, \boldsymbol{\eta}, b_\tau, T)\right\} \tag{46}$$

Then, the sensitivity of first passage probability $P_f(\boldsymbol{\theta}^{\text{I}}, \boldsymbol{\eta}, b_\tau, T)$ corresponding to uncertain parameter θ_i^{I} is defined as:

$$S(\theta_i^{\text{I}}, b_\tau) = \frac{P_f^{\text{rad}}(\boldsymbol{\theta}_i^{\text{I}}, \boldsymbol{\eta}, b_\tau, T)\,\theta_i^{\text{med}}}{\log 10\left\{P_f(\boldsymbol{\theta}^{\text{med}}, \boldsymbol{\eta}, b_\tau, T)\right\}\theta_i^{\text{rad}}} \tag{47}$$

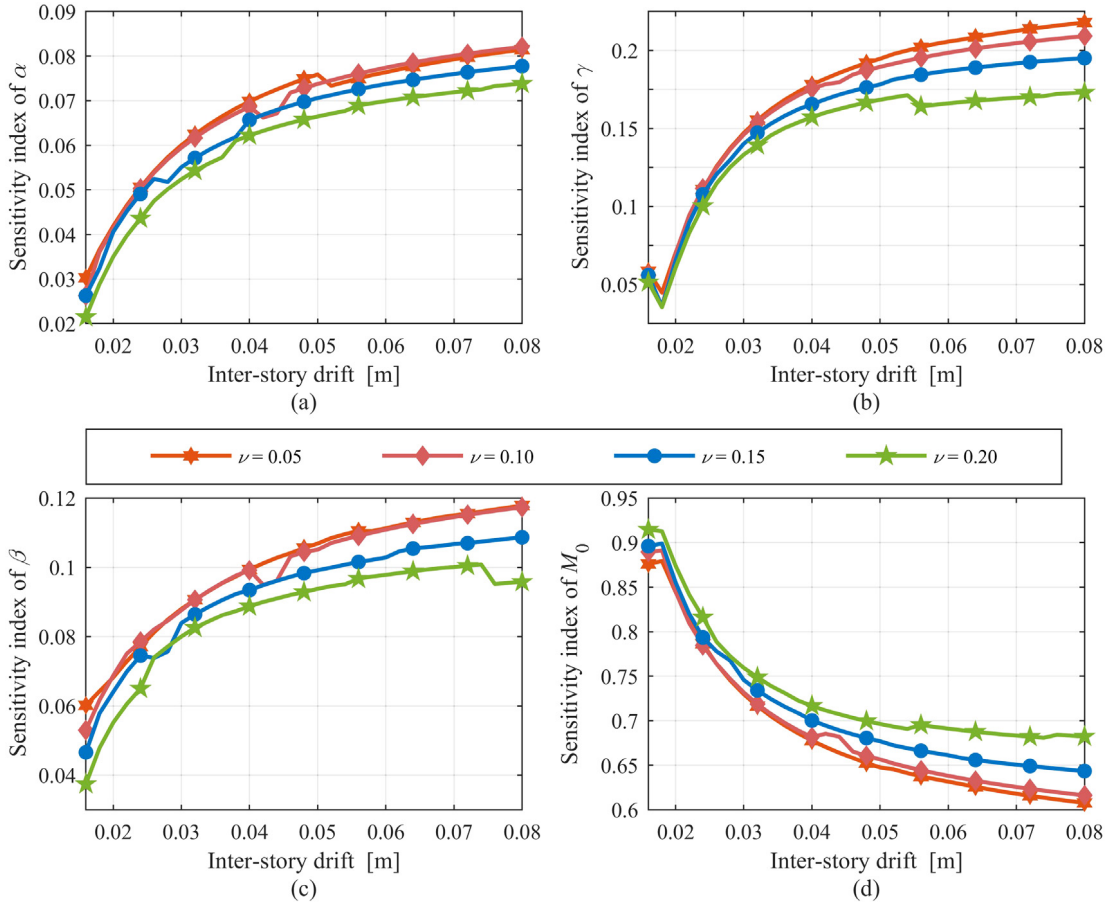

Fig. 6. Sensitivity index of uncertain parameter (a) α (b) γ (c) β and (d) M_0 with respect to the first passage probability $P_f\left(b_\tau, 15\text{ s}\right)$.

in which, $\boldsymbol{\theta}_i^{\mathrm{I}} = [\theta_1^{\mathrm{med}}, \ldots, \theta_i^{\mathrm{I}}, \ldots, \theta_n^{\mathrm{med}}]^{\mathrm{T}}$ denote the midpoint of interval vector $\boldsymbol{\theta}^{\mathrm{I}}$ except the component θ_i. The normalized sensitivity index is given by following:

$$\widetilde{S}\left(\theta_i^{\mathrm{I}}, b_\tau\right) = S\left(\theta_i^{\mathrm{I}}, b_\tau\right) / \sum_{i=1}^{d} S\left(\theta_i^{\mathrm{I}}, b_\tau\right) \tag{48}$$

The sensitivity analysis of the first passage probability $P_f\left(b_\tau, 15\text{ s}\right)$ are performed with the degree of uncertain level $\nu = 0.05,\ 0.1, 0.15$ and 0.2. The Fig. 6 shows the variation of sensitivity index with the increment of threshold value b_τ.

As shown in Fig. 6(a), (b), (c) and (d), the sensitivity index of lumped mass of structural system is much important than other three uncertain parameters. Compare the tendency of variation of sensitivity index of these four uncertain parameters with the increment of threshold value b_τ, the sensitivity of lumped mass have a negative effect on the $P_f\left(b_\tau, 15\text{ s}\right)$, while other three parameters may have positive effect on the $P_f\left(b_\tau, 15\text{ s}\right)$. This can be interpreted that the increase of lumped mass of each story may lead a high failure probability of structural system under stochastic seismic excitation. In contrast, the increase parameter α, γ and β may decrease the value of $P_f\left(b_\tau, 15\text{ s}\right)$. Moreover, the degree of importance for lumped mass is increased with the amplification of uncertain level ν, while the degree of importance for other three parameters suffered a decrease tendency with the increase of uncertain level. As reflected in Fig. 6, we can conclude that the epistemic uncertainties in lumped mass may dominated the first passage probability of structural system under stochastic excitation. To diminish the influence of epistemic uncertainties in structural system effectively, the more data or higher level of completeness of knowledge for lumped mass is necessary.

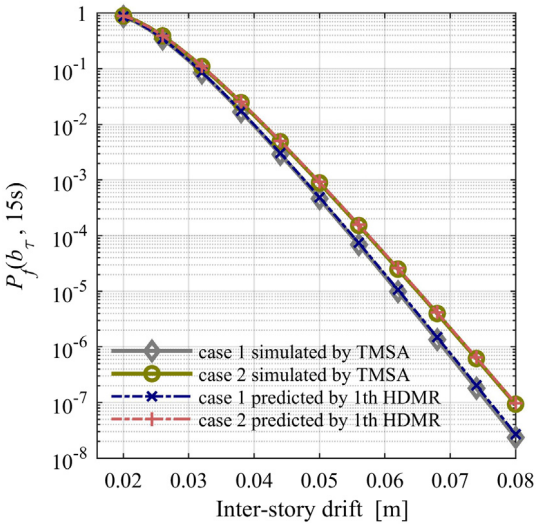

Fig. 7. Comparison the accuracy of first order HDMR prediction with uncertain level $\nu = 0.02$ of structural parameters.

6.3. Independent uncertain parameter with interval numbers

As reflected in above section, it can be found that the first order HDMR may give a well-matched approximation of first passage probability $P_f\left(b_\tau, 15\text{ s}\right)$ at the lower degree of uncertain level. Moreover, the HDMR is applicable to high dimension problems. To investigate

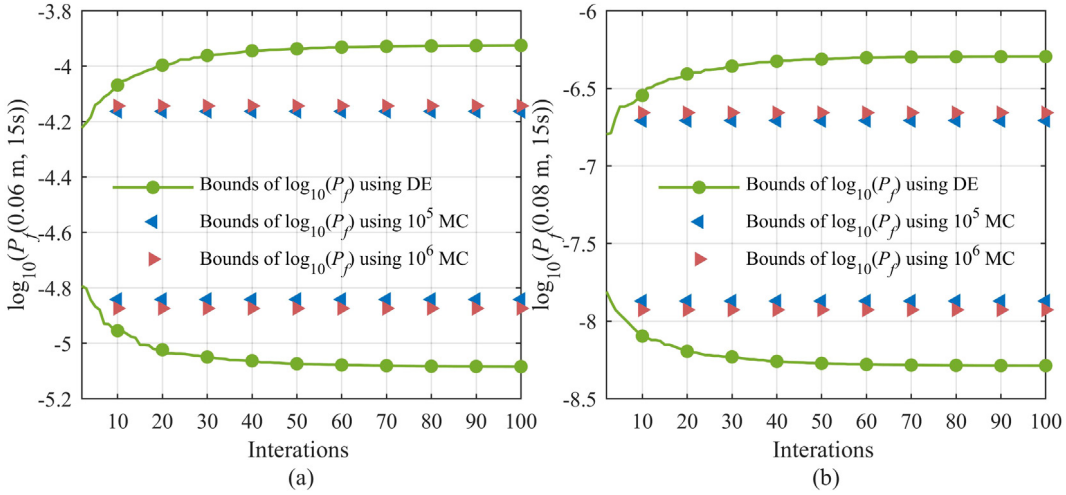

Fig. 8. The convergent history of the LB and UB of (a) $\log 10(P_f\ (0.06\ \text{m}, 15\ \text{s}))$ and (b) $\log 10(P_f\ (0.08\ \text{m}, 15\ \text{s}))$.

the performance of proposed method for high dimensional problem, the uncertain parameter in structural system are assumed as independent to each other. Then, there are 36 independent uncertain parameters of structural system shall be considered.

6.3.1. Construction and test of HDMR

In this section, the interval uncertain level ν of epistemic uncertain vector $\boldsymbol{\theta}^{\text{I}} = \left[\theta^{I}_{\mathbf{M},1}, \ldots \theta^{I}_{\mathbf{M},9}, \theta^{\text{I}}_{\alpha,1}, \ldots, \theta^{\text{I}}_{\alpha,9}, \theta^{\text{I}}_{\beta,1}, \ldots, \theta^{\text{I}}_{\beta,9}, \theta^{\text{I}}_{\gamma,1}, \ldots, \theta^{\text{I}}_{\gamma,9}\right]^{\text{T}}$ is assumed as 0.02. To investigate the accuracy of proposed method, the EVDs of case 1 and case 2 corresponding to the LB $\underline{\boldsymbol{\theta}}$ and UB $\overline{\boldsymbol{\theta}}$ of structural uncertain vector $\boldsymbol{\theta}$ are estimated by TMSA and depicted in Fig. 7, respectively.

In Fig. 7, the estimates of case 1 and case 2 predicted by HDMR are well matched with the results obtained by TMSA with 2500 CLHS simulations. Very accurate estimation of $P_f\left(b_\tau, 15\ \text{s}\right)$ demonstrates that the first order HDMR may give a good estimation of $P_f\left(b_\tau, 15\ \text{s}\right)$. Therefore, the prediction frame using first order HDMR is employed in the prediction of bounds value of first passage probability $P_f\left(b_\tau, 15\ \text{s}\right)$.

6.3.2. Estimation of the LB and UB of first passage probability

After construction the first order HDMR, we use DE interval optimization algorithm to approximate the LB and UB of $P_f\left(b_\tau, 15\ \text{s}\right)$. The initial population and maximum number of iterations are designated as 200 and 100, respectively. For investigation the convergence rate of DE, the convergent history of LB and UB of $\log 10(P_f\ (0.06\ \text{m}, 15\ \text{s}))$ and $\log 10(P_f\ (0.08\ \text{m}, 15\ \text{s}))$ are plotted in Fig. 8(a) and (b), respectively. For comparison, the quantification results obtained MC simulation with 10^5 and 10^6 sampling are also depicted in Fig. 8. The prediction results of DE and MC simulation with 10^5 and 10^6 samples are plotted in Fig. 9.

The Fig. 8(a) and (b), demonstrate the fast convergence of DE interval optimization technique. Compare to MC simulations depicted in Fig. 8(a) and (b), the DE with less than 10 iterations may present convergent solution which are certainly better than 10^5 and 10^6 MC simulation. As shown in Figs. 8 and 9, the width of the range between LB and UB of $P_f\left(b_\tau, 15\ \text{s}\right)$ computed by Monte-Carlo simulation is barely increased, while the number of samples increases from 10^5 to 10^6. In comparison, DE gives a wider range between LB and UB of $P_f\left(b_\tau, 15\ \text{s}\right)$. From above comparison, it is seemed that the DE interval optimization is very useful to search the LB and UB of $P_f\left(b_\tau, 15\ \text{s}\right)$ with good convergence. As shown in Figs. 8 and 9, the DE interval optimization gives the interval range $\left[8.24\times10^{-6}, 1.19\times10^{-4}\right]$ and $\left[5.17\times10^{-9}, 5.08\times10^{-7}\right]$ for the LB and UB of $P_f\ (0.06\ \text{m}, 15\ \text{s})$ and $P_f\ (0.08\ \text{m}, 15\ \text{s})$, respectively. It is evidently found that the small fluctuation of structural system parameters leads to a large variation of first passage probability of nonlinear system.

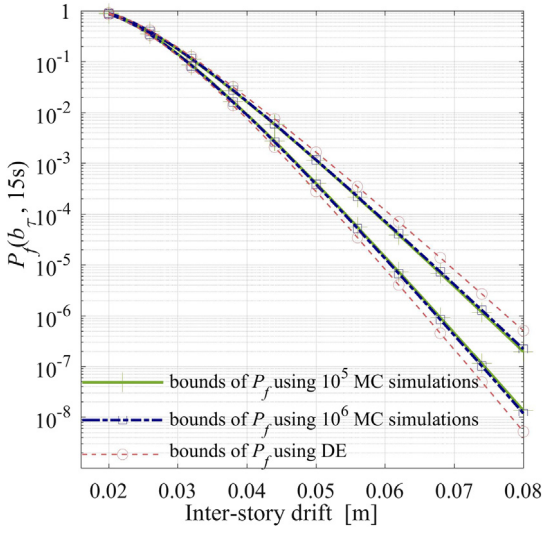

Fig. 9. Comparison the prediction of $\underline{P}_f\left(b_\tau, 15\ \text{s}\right)$ and $\overline{P}_f\left(b_\tau, 15\ \text{s}\right)$ using MC simulation with 10^5 and 10^6 samples and DE simulation with uncertain level $\nu = 0.02$ of structural parameters.

6.3.3. Sensitivity of each uncertain parameter

The sensitivity index of the $P_f\left(\boldsymbol{\theta}^{\text{I}}, b_\tau, 15\ \text{s}\right)$ are performed with the degree of uncertain level $\nu = 0.02$. The Fig. 10 shows the variation of sensitivity index for threshold value $b_\tau = 0.06$ and 0.08.

As shown in Fig. 10(a) and (b), the sensitivity index is much different from the scenario reflected from Fig. 6. On the one hand, Fig. 10(a) and (b) manifest that the importance level of $\left[\alpha_1, \ldots, \alpha_9\right]^{\text{T}}$ is smaller than 0.05, and this means the variation of $\left[\alpha_1, \ldots, \alpha_9\right]^{\text{T}}$ have a tiny impact on the variation of $P_f\left(b_\tau, 15\ \text{s}\right)$. However, the sensitivity index of $\left[\gamma_1, \ldots, \gamma_9\right]^{\text{T}}$ and $\left[\beta_1, \ldots, \beta_9\right]^{\text{T}}$ reflected in Fig. 10(a) and (b) is different from the sensitivity index shown in Fig. 6. Compare to other uncertain parameter in $\left[\gamma_1, \ldots, \gamma_9\right]^{\text{T}}$ and $\left[\beta_1, \ldots, \beta_9\right]^{\text{T}}$, the sensitivity of γ_3 and β_3 pay a more important influence on the variation of $P_f\left(b_\tau, 15\ \text{s}\right)$. The most remarkable variation is the sensitivity index of lumped mass parameter $\left[M_1, \ldots, M_9\right]^{\text{T}}$. Contrary to the analysis results demonstrated in Fig. 6, the variation of $\left[M_1, \ldots, M_9\right]^{\text{T}}$ may not dominate the first passage probability of structural system. To summarize what has been mentioned above, one reason for this scenario is the dependence of structural parameters have a prominent impact on the first passage probability of dynamic system.

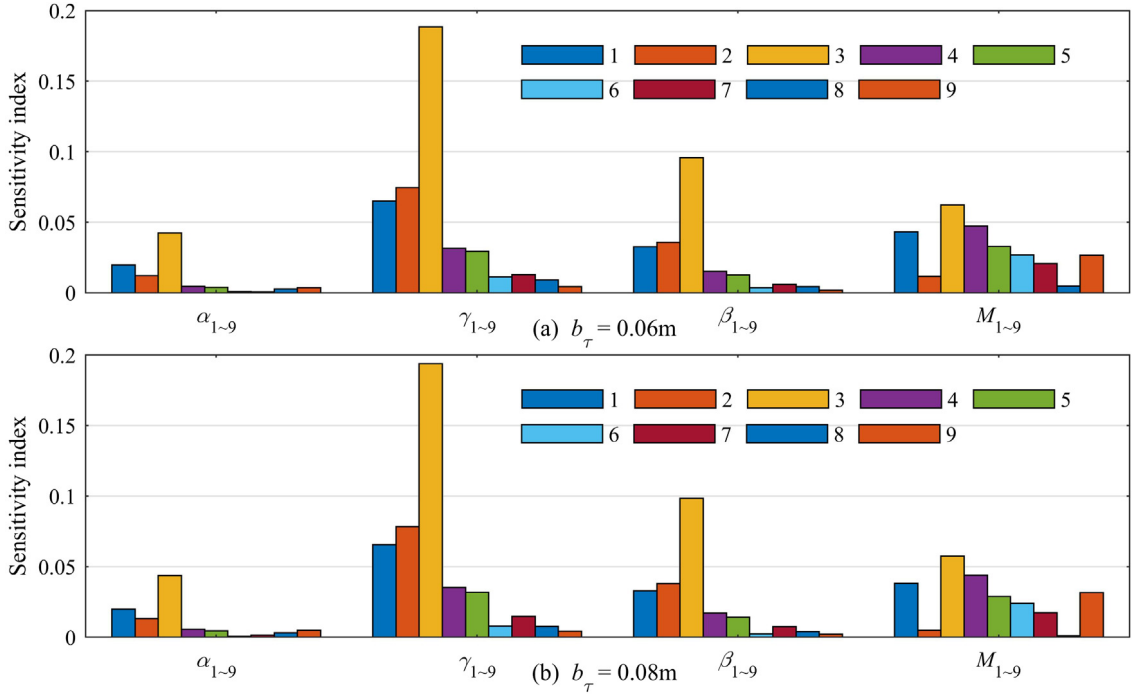

Fig. 10. Sensitivity of the first passage probability (a) P_f (0.06 m, 15 s) and (b) P_f (0.08 m, 15 s) with respect to the epistemic uncertainties in structural parameters.

7. Conclusions

This work is presented to investigate the small first passage probability of nonlinear structures with interval uncertainties under nonstationary seismic excitation. In this work, the first passage probability of the generic response process is represented by the conditional univariate EVD with interval form. The methodology involves the combination of Kriging-HDMR and TMSA is proposed to estimate the trails of the EVD of structural response for interval formed structural parameters. After the construction of meta-model, the DE based interval optimization technique is performed to search the LB and UB of first passage probability. The propagation results and convergent history shows that the DE gives a more robust quantification results than the traditional Monte-Carlo simulation. Depend on the above techniques, an interval-based sensitivity analysis is proposed to determine the importance of uncertain structural parameters. The sensitivity analysis results show that the correlation of structural uncertain parameters has an importance influence on the first passage probability of nonlinear structural system. The numerical case shows the presented methodology is efficient and high accuracy for approximation of the bounds first passage probability.

Acknowledgments

This study was supported by the Ministry of Science and Technology of China (Grant No. SLDRCE19-B-02), the National Key R&D Program of China (Grant No. 2017YFC0703607), the Natural Science Foundation of Shanghai (Grant No. 17ZR1431900), and the National Natural Science Foundation of China (Grant No. 51178337).

References

[1] S.O. Rice, Mathematical analysis of random noise, Bell Labs Tech. J. 23 (1944) 111, internal-pdf://1.1.82.65/Mathematical Analysis of Random Noise.pdf.
[2] E.H. Vanmarcke, On the distribution of the first-passage time for normal stationary random processes, J. Appl. Mech. 42 (1975) 6, http://dx.doi.org/10.1115/1.3423521.
[3] J. He, A reliability approximation for structures subjected to non-stationary random excitation, Struct. Saf. 31 (2009) 268–274, http://dx.doi.org/10.1016/j.strusafe.2008.11.001.
[4] J. He, Numerical calculation for first excursion probabilities of linear systems, Probab. Eng. Mech. 24 (2009) 418–425, http://dx.doi.org/10.1016/j.probengmech.2008.12.003.
[5] L.D. Lutes, S. Sarkani, Random Vibrations: Analysis of Structural and Mechanical Systems, Elsevier Butterworth–Heinemann, Burlington, 2004.
[6] M. Shinozuka, G. Deodatis, Simulation of stochastic processes by spectral representation, Appl. Mech. Rev. 44 (1991) 14, http://dx.doi.org/10.1115/1.3119501.
[7] M. Shinozuka, Monte CArlo solution of structural dynamics, Comput. Struct. 2 (1972) 855–874, http://dx.doi.org/10.1016/0045-7949(72)90043-0.
[8] S.K. Au, J.L. Beck, First excursion probabilities for linear systems by very efficient importance sampling, Probab. Eng. Mech. 16 (2001) 15, http://dx.doi.org/10.1016/S0266-8920(01)00002-9.
[9] J. Ching, S.K. Au, J.L. Beck, Reliability estimation for dynamical systems subject to stochastic excitation using subset simulation with splitting, Comput. Methods Appl. Mech. Engrg. 194 (2005) 23, http://dx.doi.org/10.1016/j.cma.2004.05.028.
[10] A. Naess, O. Gaidai, Estimation of extreme values from sampled time series, Struct. Saf. 31 (2009) 325–334, http://dx.doi.org/10.1016/j.strusafe.2008.06.021.
[11] C. Proppe, Equivalent linearization of MDOF systems under external Poisson white noise excitation, Probab. Eng. Mech. 17 (2002) 7.
[12] K. Fujimura, A. Der Kiureghian, Tail-equivalent linearization method for nonlinear random vibration, Probab. Eng. Mech. 22 (2007) 63–76, http://dx.doi.org/10.1016/j.probengmech.2006.08.001.
[13] M. Grigoriu, G. Samorodnitsky, Reliability of dynamic systems in random environment by extreme value theory, Probab. Eng. Mech. 38 (2014) 54–69, http://dx.doi.org/10.1016/j.probengmech.2014.08.005.
[14] J. He, Approximate method for estimating extreme value responses of nonlinear stochastic dynamic systems, J. Eng. Mech. 141 (2015) 4015009, http://dx.doi.org/10.1061/(asce)em.1943-7889.0000901.
[15] J. He, J. Gong, Estimate of small first passage probabilities of nonlinear random vibration systems by using tail approximation of extreme distributions, Struct. Saf. 60 (2016) 28–36, http://dx.doi.org/10.1016/j.strusafe.2016.02.003.
[16] J. Xu, Z. Ding, J. Wang, Extreme value distribution and small failure probabilities estimation of structures subjected to non-stationary stochastic seismic excitations, Struct. Saf. 70 (2018) 93–103, http://dx.doi.org/10.1016/j.strusafe.2017.10.007.
[17] U. Alibrandi, K.M. Mosalam, Kernel density maximum entropy method with generalized moments for evaluating probability distributions, including tails, from a small sample of data, Internat. J. Numer. Methods Engrg. (2017) http://dx.doi.org/10.1002/nme.5725.
[18] A. Der Kiureghian, O. Ditlevsen, Aleatory or epistemic? does it matter? Struct. Saf. 31 (2009) 105–112, http://dx.doi.org/10.1016/j.strusafe.2008.06.020.
[19] Y. Zhang, B. Wena, Q. Liu, First passage of uncertain single degree-of-freedom nonlinear oscillators, Comput. Methods Appl. Mech. Engrg. 165 (1998) 9, http://dx.doi.org/.

[20] A. Chaudhuri, S. Chakraborty, Reliability of linear structures with parameter uncertainty under non-stationary earthquake, Struct. Saf. 28 (2006) 231–246, http://dx.doi.org/10.1016/j.strusafe.2005.07.001.
[21] J. Li, J. Chen, W. Fan, The equivalent extreme-value event and evaluation of the structural system reliability, Struct. Saf. 29 (2007) 112–131, http://dx.doi.org/10.1016/j.strusafe.2006.03.002.
[22] V.S. Sundar, C.S. Manohar, Estimation of time variant reliability of randomly parametered non-linear vibrating systems, Struct. Saf. 47 (2014) 59–66, http://dx.doi.org/10.1016/j.strusafe.2013.10.004.
[23] G.I. Schuëller, H.J. Pradlwarter, Benchmark study on reliability estimation in higher dimensions of structural systems – An overview, Struct. Saf. 29 (2007) 167–182, http://dx.doi.org/10.1016/j.strusafe.2006.07.010.
[24] I. Elishakoff, Essay on uncertainties in elastic and viscoelastic structures: From A. M. Freudenthal's criticisms to modern convex modeling, Comput. Struct. 56 (1995) 871–895, http://dx.doi.org/10.1016/0045-7949(94)00499-S.
[25] Y. Ben-Haim, A non-probabilistic concept of reliability, Struct. Saf. 14 (1994) 227–245, http://dx.doi.org/10.1016/0167-4730(94)90013-2.
[26] L.A. Zadeh, Fuzzy sets, Inf. Control. 8 (1965) 338–353, http://dx.doi.org/10.1016/S0019-9958(65)90241-X.
[27] R.E. Moore, Interval Analysis, Prentice-Hall Englewood Cliffs, 1966.
[28] A.P. Dempster, Upper and lower probabilities induced by a multivalued mapping, Ann. Math. Stat. 38 (1967) 325–339.
[29] B. Xia, D. Yu, Modified interval and subinterval perturbation methods for the static response analysis of structures with interval parameters, J. Struct. Eng. 140 (2014) 4013113, http://dx.doi.org/10.1061/(asce)st.1943-541x.0000936.
[30] B. Xia, Y. Qin, D. Yu, C. Jiang, Dynamic response analysis of structure under time-variant interval process model, J. Sound Vib. (2016) http://dx.doi.org/10.1016/j.jsv.2016.06.030.
[31] G. Muscolino, R. Santoro, A. Sofi, Explicit reliability sensitivities of linear structures with interval uncertainties under stationary stochastic excitation, Struct. Saf. 52 (2015) 219–232, http://dx.doi.org/10.1016/j.strusafe.2014.03.001.
[32] G. Muscolino, R. Santoro, A. Sofi, Reliability assessment of structural systems with interval uncertainties under spectrum-compatible seismic excitations, Probab. Eng. Mech. 44 (2016) 138–149, http://dx.doi.org/10.1016/j.probengmech.2015.11.005.
[33] G. Muscolino, R. Santoro, A. Sofi, Reliability analysis of structures with interval uncertainties under stationary stochastic excitations, Comput. Methods Appl. Mech. Engrg. 300 (2016) 47–69, http://dx.doi.org/10.1016/j.cma.2015.10.023.
[34] D.M. Do, W. Gao, C. Song, S. Tangaramvong, Dynamic analysis and reliability assessment of structures with uncertain-but-bounded parameters under stochastic process excitations, Reliab. Eng. Syst. Saf. 132 (2014) 46–59, http://dx.doi.org/10.1016/j.ress.2014.07.002.
[35] L. Wang, X. Wang, D. Wu, X. Zhang, Non-probabilistic time-variant reliability assessment (NTRA) for the active control of vibration systems with convex uncertainties, ISA Trans. (2018) http://dx.doi.org/10.1016/j.isatra.2018.08.018.
[36] L. Wang, X. Wang, D. Wu, M. Xu, Z. Qiu, Structural optimization oriented time-dependent reliability methodology under static and dynamic uncertainties, Struct. Multidiscip. Optim. 57 (2017) 1533–1551, http://dx.doi.org/10.1007/s00158-017-1824-z.
[37] J.-B. Chen, J. Li, The extreme value distribution and dynamic reliability analysis of nonlinear structures with uncertain parameters, Struct. Saf. 29 (2007) 77–93, http://dx.doi.org/10.1016/j.strusafe.2006.02.002.
[38] C.F.J. Wu, M.S. Hamada, Experiments: planning analysis optimization, John Wiley & Sons, 2011.
[39] R. Chowdhury, B.N. Rao, A.M. Prasad, High-dimensional model representation for structural reliability analysis, Commun. Numer. Methods. Eng. 25 (2009) 301–337, http://dx.doi.org/10.1002/cnm.1118.
[40] V.U. Unnikrishnan, A.M. Prasad, B.N. Rao, Development of fragility curves using high-dimensional model representation, Earthq. Eng. Struct. Dyn. 42 (2013) 419–430, http://dx.doi.org/10.1002/eqe.2214.
[41] I. Zentner, E. Borgonovo, Construction of variance-based metamodels for probabilistic seismic analysis and fragility assessment, Georisk Assess. Manag. Risk Eng. Syst. Geohazards 8 (2014) 202–216, http://dx.doi.org/10.1080/17499518.2014.958173.
[42] S.N. Lophaven, H.B. Nielsen, J. Søndergaard, DACE-A matlab kriging toolbox, version 20, 2002.
[43] S. Guo, An efficient third-moment saddlepoint approximation for probabilistic uncertainty analysis and reliability evaluation of structures, Appl. Math. Model. 38 (2014) 221–232, http://dx.doi.org/10.1016/j.apm.2013.06.026.
[44] R. Storn, K. Price, Differential evolution–a simple and efficient heuristic for global optimization over continuous spaces, J. Global Optim. 11 (1997) 341–359, http://dx.doi.org/10.1023/A:1008202821328.
[45] H. Rabitz, Ö.F. Aliş, J. Shorter, K. Shim, Efficient input—output model representations, Comput. Phys. Comm. 117 (1999) 11–20, http://dx.doi.org/10.1016/S0010-4655(98)00152-0.
[46] J.P.C. Kleijnen, Regression and kriging metamodels with their experimental designs in simulation: A review, European J. Oper. Res. 256 (2017) 1–16, http://dx.doi.org/10.1016/j.ejor.2016.06.041.
[47] H. Tang, D. Li, J. Li, S. Xue, Epistemic uncertainty quantification in metal fatigue crack growth analysis using evidence theory, Int. J. Fatigue 99 (2017) http://dx.doi.org/10.1016/j.ijfatigue.2017.03.004.
[48] H. Tang, Y. Su, J. Wang, Evidence theory and differential evolution based uncertainty quantification for buckling load of semi-rigid jointed frames, Sadhana 40 (2015) 1611–1627, http://dx.doi.org/10.1007/s12046-015-0388-0.
[49] Y. Su, H. Tang, S. Xue, D. Li, Multi-objective differential evolution for truss design optimization with epistemic uncertainty, Adv. Struct. Eng. 19 (2016) http://dx.doi.org/10.1177/1369433216643250.
[50] K.V. Price, Differential evolution, in: Handb. Optim, Springer, 2013, pp. 187–214, internal-pdf://012324239/Differential Evolution.pdf.
[51] J. Chen, J. Li, Stochastic seismic response analysis of structures exhibiting high nonlinearity, Comput. Struct. 88 (2010) 395–412, http://dx.doi.org/10.1016/j.compstruc.2009.12.002.
[52] T.T. Baber, Random vibration of hysteretic degrading systems, J. Eng. Mech. ASCE 107 (1981) 1069–1087, https://ci.nii.ac.jp/naid/10015606921/en/.
[53] A. Olsson, G. Sandberg, O. Dahlblom, On latin hypercube sampling for structural reliability analysis, Struct. Saf. 25 (2003) 22, http://dx.doi.org/10.1016/S0167-4730(02)00039-5.